Grand-reaction method for simulations of ionization equilibria coupled to ion partitioning

Jonas Landsgesell,[†] Pascal Hebbeker,[‡] Oleg Rud,[‡] Raju Lunkad,[‡] Peter Košovan,[*,‡] and Christian Holm[*,†]

[†]*Institute for Computational Physics, University of Stuttgart, Allmandring 3, D-70569 Stuttgart, Germany*

[‡]*Department of Physical and Macromolecular Chemistry, Faculty of Science, Charles University, Hlavova 2030, 128 43 Prague, Czech Republic*

E-mail: peter.kosovan@natur.cuni.cz; holm@icp.uni-stuttgart.de

Abstract

We developed a new method for coarse-grained simulations of acid-base equilibria in a system coupled to a reservoir at a given pH and concentration of added salt, that we term the Grand-reaction method. More generally, it can be used for simulations of any reactive system coupled to a reservoir of a known composition. Conceptually, it can be regarded as an extension of the reaction ensemble, combining explicit simulations of reactions within the system and Grand-canonical exchange of particles with the reservoir. To demonstrate its strength, we applied our method to a solution of weak polyelectrolytes in equilibrium with a reservoir. Our results show that the ionization and swelling of a weak polyelectrolyte are affected by the Donnan effect due to the partitioning of ions and by the polyelectrolyte effect due to electrostatic repulsion along the chain. Both effects lead to a similar shift in ionization and swelling as a function of pH; albeit for different physical reasons. By comparison with published results,

we showed that neglecting one or the other effect may lead to erroneous predictions or misinterpretations of results. In contrast, the Grand-reaction method accounts for both effects on the results and allows us to quantify them. Finally, we outline possible extensions and generalizations of the method and provide a set of guidelines for its safe application by a broad community of users.

Introduction

Reacting systems in contact with a reservoir are ubiquitous in chemical research, especially in colloid and polymer science. Such a setup is widely used in applications to separate or purify substances[1,2], for example, in biomedical[3–5] or water purification[6–10]. Other applications include osmotic motors[11] or sensors[12]. A specific example of such a system is a solution of polyelectrolytes in a dialysis bag immersed in a reservoir solution at a given pH and salinity, as shown in Fig. 1. The dialysis bag acts as a semipermeable membrane that prevents polyelectrolytes from escaping and simultaneously allows the exchange of small ions. Functionalized nanoparticles, proteins, or any other colloids in a solution separated by a semipermeable membrane from the reservoir would be described similarly. If the polyelectrolyte contains weak acid groups, they undergo the following ionization reaction

$$\mathrm{HA} \rightleftharpoons \mathrm{A}^- + \mathrm{H}^+ \tag{1}$$

The equilibrium state of this reaction is determined by the pH and by the activity of other ions in the system. The presence of charged polymers affects the partitioning of exchangeable ions between the system and the reservoir, particularly affecting the concentration of H^+ ions in the system. Changing ion concentrations affect the reaction equilibrium, which in turn affects the ion partitioning in a complicated feedback loop. To represent such a system in a molecular simulation, this feedback loop must be described correctly.

Another example of a reacting system in equilibrium with a reservoir is a weak poly-

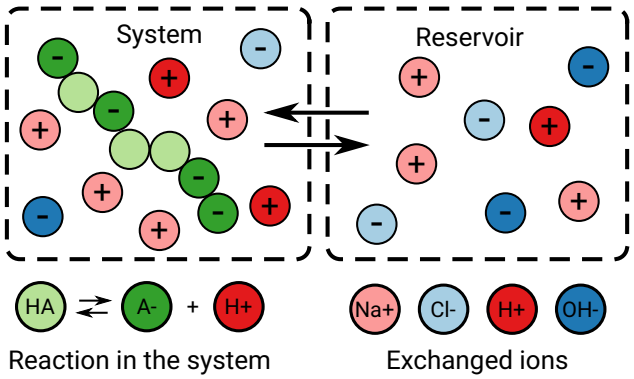

Figure 1: Schematic illustration of the investigated system: A weak polyelectrolyte solution in equilibrium with a reservoir at a given pH and salinity. The weak polyelectrolyte undergoes an acid-base ionization reaction with the H^+ ions present in the system. Some ions are exchanged between the system and the reservoir, while the polyelectrolyte is present only in the system. Due to the Donnan partitioning, the concentrations of exchangeable ions and the pH differ between the system and the reservoir.

electrolyte hydrogel immersed in a salt solution. The partitioning of salt ions and H^+ ions affects the swelling of polyelectrolyte hydrogels and is coupled to the ionization degree of the polyelectrolyte. The ionization degree determines their ability to capture or release ions at various pH values, which is relevant in desalination, controlled release and water treatment applications[9,10]. Semipermeable membranes are not necessary for such systems because gel connectivity prevents the polymer from escaping the gel phase without affecting its ability to exchange ions with the surrounding reservoir solution. Similarly to gels, partitioning of salt ions affects the stability of phase-separated complex coacervates[2,13–16]. The envisioned application of coacervates to the separation of charged proteins[2] requires understanding the partitioning between the coacervate and the supernatant solution, while protein release by a change in pH depends on the acid-base ionization equilibrium in the coacervate, which is inherently coupled to the partitioning of H^+ ions. Salt solutions in equilibrium with polymer brushes, vesicles, or micelles could also be described similarly.

The Donnan theory qualitatively explains the coupling between the ion partitioning and the ionization degree, by assuming an ideal (non-interacting) system but imposing the electroneutrality constraint. In general, the Donnan partitioning of H^+ ions suppresses the ion-

ization degree of a weak polyelectrolyte, which we will call the Donnan effect[17,18]. In contrast to the Donnan effect, charge-charge repulsion in polyelectrolytes suppresses their ionization as a consequence of strong electrostatic interactions between nearby ionized groups[19–25]. A similar effect is well known in the pH-dependent ionization of charged colloids or proteins[26–29]. Although the resulting shift in ionization response is qualitatively similar to the Donnan effect, this shift originates from electrostatic interactions in a system, irrespective of ion partitioning, and is absent without interactions. To distinguish this effect of interactions from the Donnan effect, we will call it the polyelectrolyte effect.

Based on the above and to our best knowledge, a theory or a simulation method efficiently combining the Donnan effect with the polyelectrolye effect does not yet exist despite its importance for solving many problems. The challenge in simulating such a system is deciding on how to combine a method for simulating chemical reactions with a method for simulating the exchange of particles with the reservoir. Although simulation methods for each of these problems are available, combining them in one simulation is a complicated task. To underpin the challenge, we briefly describe some of the aforementioned methods, highlighting their main approximations, limitations and possible artefacts.

Simulations in the Grand-canonical ensemble account for the coupling of a simulated system with a reservoir. In its most common implementation[30], one particle of the exchanged species is inserted in, or deleted from, the simulation box. This change is accepted or rejected in a Monte-Carlo scheme with an acceptance probability that depends on the chemical potential of the exchanged species in the reservoir and on the interactions in the simulation box. When exchanging ionic species with the reservoir, inserting a single ion creates a non-neutral simulation box. In the most commonly used periodic boundary conditions, such an insertion results in an infinite energy change; and this insertion should always be rejected. The problem of electroneutrality can be overcome by exchanging an ion pair, or more generally an electroneutral group of cations and anions. In such a case, fluctuations in the ionic composition are allowed, without affecting the electroneutrality. Non-reactive simple elec-

trolyte solutions[31], polyelectrolyte solutions[32–34] and polyelectrolyte hydrogels[35–39] coupled to a salt solution reservoir have been simulated in this way. In a real system, electroneutrality does not have to be strictly obeyed at a nanoscale, and imposing the electroneutrality constraint artificially prevents some fluctuations. Therefore, Barr and Panagiotopoulos[33] proposed relaxing the electroneutrality constraint using a modified calculation of the electrostatic interaction energy, which yields a high but finite energy of a non-neutral simulation box. Then, insertions and deletions of individual ions are allowed as the system remains electroneutral on average. Regardless of how electroneutrality is treated, the Grand-canonical coupling described above accounts for composition fluctuations due to Donnan partitioning of ions but not for those due to chemical reactions involving those species in the system, which cannot be exchanged with the reservoir.

To simulate chemical reactions in a closed system uncoupled to a reservoir, we can use the Reaction-ensemble Monte Carlo[40–42] (RxMC) or the Constant-pH[43] (cpH) algorithm. Various weak polyelectrolyte systems have been simulated using the RxMC method[24,44–48] or cpH method[25,49–57]. In RxMC[40], we simulate chemical reactions by inserting and deleting particles, or by changing their chemical identity, as prescribed by the stoichiometry of the simulated reaction. Chemical equilibrium is achieved by performing the reaction moves in the forward and reverse directions of the reaction and by accepting the moves with a Metropolis-like acceptance probability. Ionization in RxMC simulations of polyelectrolytes is varied by varying its acidity constant, while the solution pH results from the simulation. The constant-pH method has been introduced to enable simulations of acid-base ionization reactions at a given pH[43]. Unlike RxMC, the pH of the system is an input parameter of the cpH method, and directly enters the acceptance probability of the reaction move. However, it is not explicitly coupled to the actual number of H^+ ions in the simulation box, which may lead to artefacts in specific situations[58,59]. Explicit coupling of the constant-pH method to a reservoir is not straightforward because the pH of the system is needed as an input parameter, but its relation to the pH of the reservoir is not known a priori. Explicit coupling

of the RxMC method to the reservoir is a seemingly easier approach. However, this method becomes highly inefficient when the number of particles of one or more reacting species is low. This limitation concerns especially H^+ and OH^- ions when simulating acid-base equilibria close to pH = 7, because their concentration is very low[58,60,61]. Thus, combining these methods for simulating reactive systems coupled to a reservoir is a complicated task.

Reactive systems coupled to a reservoir have been studied in the past, mostly by using mean-field models and a partial-open ensemble[62]. The mean-field approximation represents discrete particles by a density field (continuum), proportional to the average probability of finding a particle in a given region of space. A density distribution that minimizes the free energy functional is then sought, for example, by solving the Poisson-Boltzmann equation[63], or a similar equation that also accounts for non-electrostatic interactions[17,18,64–70]. This approximation inherently neglects some correlations but simultaneously renders the computational cost relatively insensitive to the actual number of particles in the studied system. Such an approach has been used to study various systems in equilibrium with a bulk solution, such as proteins treated as rigid objects[27,71], flexible star-like polymers[17,66,67,72,73], or planar systems, including a polyelectrolyte brush grafted to a surface[68,70,74–76]. Polyelectrolyte hydrogels have been studied using a similar approach[18,69,77–79]. Coupling to the reservoir in the partial-open ensemble can be achieved by setting suitable boundary conditions sufficiently far from the object of interest (colloidal particle or polymer) and by explicitly accounting for density gradients at the system-reservoir interface. Specifically, the pH and the concentrations of ions in the reservoir enter the mean-field models as a boundary condition for the Poisson-Boltzmann (PB) equation. Then, the Donnan potential and electroneutrality of the whole system follow as consequences of self-consistent determination of the electrostatic potential. Chemical equilibria in mean-field models are determined by the local concentrations of reacting species, coupled to the PB equation. To alleviate some limitations of mean-field representation, studies have combined explicit-particle simulations with the mean-field representation of exchangeable ions[70,80–84], thereby coupling the exchangeable ions to the

reservoir, as usually performed in the mean-field.

In contrast to the number of mean-field or mixed field+particle representations, coarse-grained simulations of reactive systems explicitly coupled to a reservoir are scarce. Johnson et al.[41] were the first to propose an extension of the reaction ensemble by combining it with the Gibbs ensemble to simulate phase equilibria. Interestingly, even though their article has been cited many times, this aspect of their work seems overlooked. To some extent, their approach closely resembles the Grand-reaction method presented in this manuscript. However, they focused on simulations of neutral systems in situations with equal pressures in both simulation boxes. Moreover, they were not concerned with multi-component reaction equilibria at which some of the reacting species have very low concentrations or with situations where some reactive species might not be exchanged. Recent simulations of weak polyelectrolytes by Rathee et al.[60,61] also closely resemble our method. However, their coupling to the multi-component reservoir was incomplete, which may lead to artefacts under specific conditions. In addition, their simulation setup was inefficient in simulating reactions close to neutral pH, which is relevant in many applications. Thus, a robust simulation method for coarse-grained simulations of acid-base ionization equilibria coupled to a reservoir at an arbitrary pH has not been developed yet.

The Grand-reaction method, presented here, couples the Reaction-ensemble treatment of the acid-base reactions and the Grand-canonical exchange of ions with a reservoir of a specific composition. Below, we describe the simulation protocol and provide a set of guidelines to ensure that the imposed pH and the numbers of all ions in the simulation box are consistent with the reservoir composition. In principle, the Grand-reaction method enables simulations at an arbitrary combination of pH and amount of added salt. In practice, this means that the accessible pH range is no longer limited by the simulation algorithm; it is only limited by the computational power, and by the quality of the model used to represent the ions and colloidal particles in the implicit solvent. Furthermore, the method can be generalized to other chemical reactions and other types of reservoirs.

Theoretical Background

To introduce the notation and terminology, we briefly recapitulate the main concepts in describing the Donnan equilibria and chemical reaction equilibria. This is particularly important to avoid ambiguity in various notation conventions apparently used in literature. We start by describing ideal systems without intermolecular interactions and then extend them to interacting systems.

Donnan Contribution to the Chemical Potential

We define the extended chemical potential μ of species i as

$$\mu_i = \mu_i^{\ominus} + \mu_i^{\mathrm{id}} + \mu_i^{\mathrm{ex}} + z_i \mu^{\mathrm{don}} \tag{2}$$

where z_i is the valency of species i. We choose the convention that the reference chemical potential $\mu^{\ominus}$ is the chemical potential of an ideal gas at reference concentration $c^{\ominus} = 1\,\mathrm{M}$. The ideal contribution μ_i^{id} is defined as

$$\mu_i^{\mathrm{id}} = k_{\mathrm{B}} T \ln\left(c_i / c^{\ominus}\right) \tag{3}$$

where c_i is the concentration of species i. The excess contribution μ_i^{ex} arises due to intermolecular interactions, therefore $\mu^{\mathrm{ex}} = 0$ for a non-interacting system. The Donnan contribution μ^{don} arises when minimizing the total free energy of (system + reservoir) under the electroneutrality constraint (see Supporting Information, Section S4), such that $\mu^{\mathrm{don}} = 0$ in the reservoir. The Donnan potential exactly cancels for any group of exchangeable ions that is overall electroneutral because $\sum_i z_i \mu^{\mathrm{don}} = \mu^{\mathrm{don}} \sum_i z_i = 0$. With the definition in Eq. 2, the extended chemical potentials are equal in the system and in the reservoir. We use the term extended to emphasize that our definition of the chemical potential includes the Donnan term, which is usually omitted. This term must be accounted for when considering

chemical reactions inside the system, involving constituents exchanged with the reservoir. The μ^{don} term leads to partitioning of ions between the system and the reservoir that is commonly known as Donnan partitioning[85–87].

The activity, a, can be defined in analogy with Eq.3, as:

$$\mu_i^{\mathrm{id}} + \mu_i^{\mathrm{ex}} = k_{\mathrm{B}} T \ln a_i \tag{4}$$

which is also used in the IUPAC definition of pH[88],

$$\mathrm{pH} = -\log_{10} a_{\mathrm{H^+}} = -\frac{1}{k_{\mathrm{B}} T \ln(10)} \left(\mu_{\mathrm{H^+}}^{\mathrm{id}} + \mu_{\mathrm{H^+}}^{\mathrm{ex}}\right) \tag{5}$$

In practice, the activity of a single ion cannot be measured. The pH measurement in the system actually yields the activity of an ion pair[89]. In the chemical potential of an ion pair, the Donnan contributions of the individual ions cancel each other. Therefore, the definition of activity does not include the Donnan potential, and the values of pH measured in the system and in the reservoir differ by the Donnan term:

$$\mathrm{pH}_{\mathrm{sys}} = \mathrm{pH}_{\mathrm{res}} + \frac{\mu^{\mathrm{don}}}{k_{\mathrm{B}} T \ln(10)} \tag{6}$$

Eq. 6 shows that a negative value of μ^{don} implies $\mathrm{pH}_{\mathrm{sys}} < \mathrm{pH}_{\mathrm{res}}$, and a positive value of μ^{don} implies $\mathrm{pH}_{\mathrm{sys}} > \mathrm{pH}_{\mathrm{res}}$. Because we are mostly concerned with pH in the reservoir, we introduce the convention that from now on pH without superscript always denotes the pH measured in the reservoir. However, we keep the subscript whenever it is necessary to distinguish the two contributions in one equation.

Donnan equilibrium with four ionic species

In Section S4, in the Supporting Information, we show that the partitioning of ions in a system with four ionic constituents exchanged with the reservoir is described by the same

equations as those used in the original Donnan description[85], which has been formulated for a two-component system in equilibrium with a one-component reservoir consisting of only the salt ions (NaCl). The only difference is that the salt concentration in the original formulation must be replaced by the reservoir ionic strength, I^{res}. In this treatment, all species are treated as an ideal gas, with an additional constraint due to electroneutrality, requiring that the chemical potentials of each mobile species be equal in the system and in the reservoir, which leads to the well-known Donnan equations. The partition coefficient ξ_i of species i is defined as the ratio of its concentrations in the system and in the reservoir

$$\xi_i = \frac{c_i^{\mathrm{sys}}}{c_i^{\mathrm{res}}} = \exp\left(-\frac{z_i \mu^{\mathrm{don}}}{k_{\mathrm{B}} T}\right) \tag{7}$$

This can be expressed as

$$\xi_{\mathrm{i}} = \frac{c_i^{\mathrm{sys}}}{c_i^{\mathrm{res}}} = \frac{z_i c_{\mathrm{A}^-}}{2I^{\mathrm{res}}} + \sqrt{\left(\frac{c_{\mathrm{A}^-}}{2I^{\mathrm{res}}}\right)^2 + 1} \tag{8}$$

where I^{res} denotes the ionic strength in the reservoir, defined as

$$I^{\mathrm{res}} = \frac{1}{2}\sum_i z_i^2 c_i^{\mathrm{res}} \tag{9}$$

We use the same formula to define the ionic strength in the system, but in this case the summation runs only over exchangeable ions, that is, it excludes the charges on the poly-electrolyte.

Reaction equilibrium in a system coupled to a reservoir

Consider a general chemical reaction, defined by the stoichiometry:

$$\nu_{\mathrm{A}}\mathrm{A} + \nu_{\mathrm{B}}\mathrm{B} \rightleftharpoons \nu_{\mathrm{C}}\mathrm{C} + \nu_{\mathrm{D}}\mathrm{D} \tag{10}$$

where ν_A is the stoichiometric coefficient of species A and analogously for all other species. Equation 10 can be rewritten as $\sum_i \nu_i \mathrm{X}_i = 0$, which uses the convention that $\nu < 0$ for the reactants (species on the left-hand side of Eq. 10) and $\nu > 0$ for products (species on the right-hand side of Eq. 10). The corresponding equilibrium constant is defined as

$$k_\mathrm{B} T \ln K = -\sum_i \nu_i \mu_i^\ominus \tag{11}$$

Chemical equilibrium requires that $\sum_i \nu_i \mu_i = 0$, which allows us to express K as

$$k_\mathrm{B} T \ln K = \sum_i \nu_i (\mu_i - \mu_i^\ominus) = \sum_i \nu_i (\mu_i^\mathrm{id} + \mu_i^\mathrm{ex} + z_i \mu^\mathrm{don}) \tag{12}$$

For reactions without changes in total charge, the Donnan contributions in Eq. 12 exactly cancel each other. To demonstrate that this is indeed true, we can consider the following thought experiment: First, let a system in contact with a reservoir reach equilibrium. Then, create a closed system by removing the reservoir and by preventing further exchanges. Removing the reservoir has no effect on the system composition and therefore on the chemical equilibrium. The reaction equilibrium in this closed system depends on the concentrations of individual species but not on the Donnan potential. Thus, the reaction equilibrium in the system with the reservoir cannot explicitly depend on the Donnan potential either. Instead, the Donnan potential affects the partitioning of all exchangeable ions and therefore the overall composition. This change in composition then affects the chemical equilibrium of reactions in which some ionic species cannot be exchanged. When applying these considerations to the acid-base ionization reaction in Eq.1, we derive the Henderson-Hasselbalch equation in the form

$$\log_{10}\left(\frac{\alpha}{1-\alpha}\right) \overset{\text{ideal}}{=} \mathrm{pH}_\mathrm{sys} - \mathrm{p}K_\mathrm{A} = \mathrm{pH}_\mathrm{res} - \mathrm{p}K_\mathrm{A} + \frac{\mu^\mathrm{don}(\alpha)}{k_\mathrm{B} T \ln(10)} \tag{13}$$

where $\alpha = c_{\mathrm{A}^-}/(c_{\mathrm{A}^-} + c_{\mathrm{HA}})$ is the ionization degree of the acid; by writing $\mu^{\mathrm{don}}(\alpha)$, we emphasize that the Donnan contribution depends on α. Eq. 7 and Eq. 8 imply that if the non-exchanged species is an anion A^-, then $\mu^{\mathrm{don}} < 0$ and $\mathrm{pH}_{\mathrm{sys}} < \mathrm{pH}_{\mathrm{res}}$. Therefore, the Donnan partitioning decreases the ionization of the weak acid in the system in comparison with the ionization in the reservoir. Conversely, if the non-exchanged species is a weak base, then $\mu^{\mathrm{don}} > 0$ and $\mathrm{pH}_{\mathrm{sys}} > \mathrm{pH}_{\mathrm{res}}$, again resulting in a decreased ionization. In an ideal non-interacting system, only the Donnan contribution shifts the ionization equilibrium. In an interacting system, both ionization equlibrium and Donnan partitioning are affected by the interactions. One of the objectives of our work is to quantify the magnitude of these contributions under various conditions.

Extension to non-ideal systems

All the above considerations can be easily extended to non-ideal interacting systems by explicitly accounting for inter-particle interactions, which only affect the excess chemical potentials. The excess chemical potentials are non-zero in an interacting system, and they do not cancel for oppositely charged ions. Conversely, they tend to have the same sign and they also have the same magnitude if the system is symmetric with respect to the sign of all charges. This is an important difference between the excess contribution and the Donnan contribution, which is also non-zero in an ideal system and exactly cancels for an electroneutral group of ions.

Method

Required Input Parameters

The Grand-reaction method (G-RxMC) introduced in this work provides a general approach to simulating multi-component reaction equilibria. We focus on coarse-grained models representing an aqueous solution of ions in an implicit solvent that is treated as a continuum,

characterized by the relative permittivity, ε_r. We define the system by specifying its temperature T, volume V, concentrations c of components that cannot be exchanged with the reservoir, and chemical potentials μ of those components that the system can exchange with the reservoir. Alternatively, we can specify concentrations of the reservoir constituents and determine their chemical potentials. Furthermore, we specify the chemical reactions that occur in the system by their stoichiometry and by their equilibrium reaction constants K. We follow the IUPAC nomenclature[90] to distinguish constituents of the system (all distinct chemical species present in the system) and the components (constituents, whose concentration of which can be varied independently). In the general case, the reservoir may consist of an arbitrary number of constituents, and the chemical reactions can involve arbitrary constituents of the system.

In the example described below, we apply this general framework to a solution of weak polyelectrolytes composed of N identical segments, in equilibrium with a salt solution at a given pH and composition. In this example, the polymer chains represent the components that are not exchanged with the reservoir, whereas the H^+, Na^+, Cl^-, and OH^- ions represent the constituents that are exchanged with the reservoir. In general, in a reservoir containing n ionic constituents, only $(n-1)$ chemical potentials can be specified independently. The chemical potential of the last constituent is determined by the electroneutrality constraint, and this constituent is sometimes termed neutralizer[44,91]. In addition, the chemical potentials of H^+ and OH^- are coupled by the ionic product of water, which provides a second constraint. Therefore, in aqueous solutions only $(n-2)$ chemical potentials can be specified independently. Chemical reactions in our system comprise the acid-base ionization of the weak polyelectrolyte, characterized by the acidity constant K_A. All involved constituents are described by short-range repulsive interaction potentials (to account for excluded volume) and by the valency (which determines their electrostatic interactions). Polymer connectivity is further characterized by an anharmonic bonding potential. Full details of the simulation setup are given in the Supporting Information, Section S1.1 and Section S3.

The simulation comprises a Monte Carlo (MC) procedure. This procedure samples the simulated system in several orthogonal dimensions: (i) sampling particle positions while maintaining a fixed composition; and sampling composition fluctuations due to (ii) chemical reactions and to (iii) exchange of particles with the reservoir. Particle positions (displacement moves) can be sampled using the standard Monte Carlo (MC) schemes or stochastic dynamics algorithms[58]. These procedures are well established, and thus we will not discuss them in detail. The moves accounting for chemical reactions (reaction moves) and the moves accounting for exchange of particles with the reservoir (particle exchange moves) are crucial for our method. Therefore, we will discuss them in detail below.

Accounting for Chemical Reactions

We used the reaction ensemble algorithm (RxMC) to account for chemical reactions taking place in the system and for the exchange of particles between the system and the reservoir. The RxMC method has been originally formulated for closed systems. To highlight that our approach considers exchanges with a reservoir, we have designated it the Grand-reaction method. The RxMC method defines the corresponding acceptance probability for the transition between the old state (o) and the new state (n) of a general reaction, Eq.10[40,42,58]:

$$P_{\mathrm{on}}^{\mathrm{RxMC}} = \min\left\{1, \left(K\left(c^{\ominus}VN_{\mathrm{A}}\right)^{\bar{\nu}}\right)^{\xi} \prod_i \left[\frac{(N_i^0)!}{(N_i^0+\nu_i\xi)!}\right] \exp\left(-\beta\Delta U_{\mathrm{on}}\right)\right\} \tag{14}$$

where $\bar{\nu} = \sum_i \nu_i$, and N_{A} is the Avogadro number. The extent of reaction $\xi = 1$ corresponds to the forward direction (left to right) of the reaction in Eq. 10, and $\xi = -1$ corresponds to the reverse direction. Note that the assumption of an implicit solvent implies that both reactants and products in Eq. 10 are solvated molecules. Therefore, the equilibrium constant K corresponds to the chemical reactions in solutions, whereas the original formulation of the reaction ensemble[40] considered equilibrium constants of gas-phase reactions. The tabulated equilibrium constants for gas-phase reactions and solution reactions are related to each other

by a constant factor that must be considered when performing quantitative predictions. The conversion of the tabulated equilibrium constants for aqueous solutions into inputs of the implicit-solvent simulations is described in the appendix of Ref[58].

Acid/Base Ionization Reaction

Acid-base ionization equilibria involve a reaction with water, while water molecules are not treated explicitly in the implicit-solvent representation. This requires special caution when setting-up the reactions. The acidity constant, K_{A}, is the equilibrium constant of the ionization reaction in Eq. 1

$$k_{\mathrm{B}}T \ln K_{\mathrm{A}} = \mu^{\ominus}_{\mathrm{HA}} - \mu^{\ominus}_{\mathrm{H^+}} - \mu^{\ominus}_{\mathrm{A^-}} \tag{15}$$

By convention, the chemical potential of water is assumed to be constant and included in the definition of K_{A}. This is consistent with the implicit solvent representation assumed in our simulation method. Although the water molecules are not represented by explicit particles, they participate in the acid-base ionization, and the $\mathrm{H^+}$ and $\mathrm{OH^-}$ ions produced by the ionization reactions must be represented explicitly.

The acid ionization reaction, Eq. 1, can be conveniently simulated using the reaction ensemble at pH $\lesssim 4$. At pH $\gtrsim 4$, the concentration of $\mathrm{H^+}$ is so low that with a typical simulation box size, $L \approx 20\,\mathrm{nm}$, one obtains less than one $\mathrm{H^+}$ ion per simulation box, and the reaction ensemble simulation becomes very inefficient. At pH $\gtrsim 10$, this problem can be circumvented by re-formulating the ionization reaction using the $\mathrm{OH^-}$ ion instead of $\mathrm{H^+}$, as shown by Rathee et al.[60,61]. However, both $\mathrm{H^+}$ and $\mathrm{OH^-}$ ions are scarce in the intermediate pH range. In this case, sampling the ionization reaction using a similar approach would cause a bottleneck in the whole simulation.

To avoid this bottleneck, we re-formulated the ionization reaction using other ions, and modified the equilibrium constants accordingly. By using the reaction in Eq. 1 and by adding

or subtracting the chemical potentials or ions exchanged with the reservoir, we obtain

$$\mathrm{HA} \rightleftharpoons \mathrm{A^-} + \mathrm{H^+}, \qquad k_\mathrm{B}T \ln K_\mathrm{A} = -\mu^\ominus_{\mathrm{A^-}} - \mu^\ominus_{\mathrm{H^+}} + \mu^\ominus_{\mathrm{HA}} \tag{16}$$

$$\mathrm{HA} + \mathrm{OH^-} \rightleftharpoons \mathrm{A^-}, \qquad k_\mathrm{B}T \ln K'_\mathrm{A} = -\mu^\ominus_{\mathrm{A^-}} - \mu^\ominus_{\mathrm{H^+}} + \mu^\ominus_{\mathrm{HA}} - k_\mathrm{B}T \ln K_\mathrm{w} \tag{17}$$

$$\mathrm{HA} \rightleftharpoons \mathrm{A^-} + \mathrm{Na^+}, \qquad k_\mathrm{B}T \ln K''_\mathrm{A} = -\mu^\ominus_{\mathrm{A^-}} + \mu^\ominus_{\mathrm{HA}} + \mu_{\mathrm{Na^+}} - \mu^\ominus_{\mathrm{Na}} - \mu_{\mathrm{H^+}} \tag{18}$$

$$\mathrm{HA} + \mathrm{Cl^-} \rightleftharpoons \mathrm{A^-}, \qquad k_\mathrm{B}T \ln K'''_\mathrm{A} = -\mu^\ominus_{\mathrm{A^-}} + \mu^\ominus_{\mathrm{HA}} - \mu_{\mathrm{H^+}} - \mu_{\mathrm{Cl^-}} + \mu^\ominus_{\mathrm{Cl}} \tag{19}$$

The reactions Eq. 17–19 can be formally derived as the net result of combining Eq. 16, representing the ionization reaction, with Eq. 21–24, representing the ion-exchange with the reservoir, as defined in the next section. Note that only K_A and K'_A are true equilibrium constants because they are independent of the reservoir composition, whereas the constants K''_A and K'''_A depend on the reservoir composition.

Finally, the ionization reaction must be coupled to the ion-exchange reaction with the reservoir. Otherwise, the reaction equilibrium will not account for the Donnan partitioning of ions, which would occur if we used the constant-pH method[43] for simulating the ionization equilibrium. The constant-pH method uses the pH in the system as input parameter, and the ionization reaction is not directly coupled to the number of $\mathrm{H^+}$ ions in the simulation box. This method accounts for the ideal-gas contribution ($\mu^\mathrm{id}_{\mathrm{H^+}}$) to the chemical potential of $\mathrm{H^+}$ and for contributions due to two-body interactions ($\mu^\mathrm{ex}_{\mathrm{H^+}}$) but not for the Donnan contribution to $\mu_{\mathrm{H^+}}$ and to the pH. Therefore, the constant-pH method cannot be used to simulate a system in equilibrium with a reservoir.

Connecting the System to the Reservoir

Exchanging Particles with the Reservoir

To couple the simulated system to the reservoir, we implemented the Grand-canonical particle exchange, using the acceptance probability[30,92]:

$$P_{\text{on}}^{\text{GCMC}} = \min\left\{1, \left(\prod_i \left[\frac{N_i^0! V c^{\ominus}}{(N_i^0 + \nu_i \xi)!}\right]^{\nu_i \xi}\right) \exp\left(\beta\left[\xi \sum_i \nu_i(\mu_i - \mu_i^{\ominus}) - \Delta U_{\text{on}}\right]\right)\right\} \quad (20)$$

The summation and the product in the acceptance probability both run over all constituents exchanged in this move. For insertions, $\xi = +1$, whereas for deletions, $\xi = -1$. The stoichiometric coefficients ν_i determine the number of particles of constituent i exchanged during the move (see also Eq. 21–Eq. 27).

Formally, we can write these particle insertions and deletions as chemical reactions in which particles are created (inserted) in the simulation box or removed (deleted) from the simulation box. To retain the electroneutrality of the simulation box, we always insert or delete an electroneutral ion pair. Specifically, to simulate particle exchange with a reservoir consisting of Na^+, Cl^-, H^+ and OH^- ions, we define the following reactions (ion pair insertions):

$$\emptyset \rightleftharpoons Na^+ + Cl^-, \qquad K_{\text{Na+Cl}} \quad (21)$$

$$\emptyset \rightleftharpoons H^+ + Cl^-, \qquad K_{\text{H+Cl}} \quad (22)$$

$$\emptyset \rightleftharpoons Na^+ + OH^-, \qquad K_{\text{Na+OH}} \quad (23)$$

$$\emptyset \rightleftharpoons H^+ + OH^-, \qquad K_{\text{H+OH}} \equiv K_{\text{w}} \quad (24)$$

where K_{w} is the ionic product of water, and we define the remaining equilibrium constants in Equations 21 to 24 as $k_{\text{B}}T \ln K_{i+j} = (\mu_i - \mu_i^{\ominus}) + (\mu_j - \mu_j^{\ominus})$. The above equations are not independent because adding (Eq. 21 + Eq. 24) is equivalent to adding (Eq. 23 + Eq. 22), thereby resulting in the following stoichiometry constraint, equivalent to imposing electroneutrality

of the reservoir:

$$K_{\mathrm{Na+Cl}} K_{\mathrm{w}} = K_{\mathrm{H+Cl}} K_{\mathrm{Na+OH}} \tag{25}$$

Since K_{w} is fixed, only two of the three remaining constants can be chosen independently to uniquely determine the system composition. In our case, we specify the remaining two degrees of freedom by setting the pH and the concentration of added salt in the reservoir.

As an alternative to inserting or deleting ion pairs, particle identities can be exchanged, which is formulated as reactions formally derived by subtracting (Eq. 23 − Eq. 24) and (Eq. 22 − Eq. 24)

$$\mathrm{H^+} \rightleftharpoons \mathrm{Na^+} \qquad K_{\mathrm{Na-H}} = K_{\mathrm{Na+OH}}/K_{\mathrm{w}} \tag{26}$$

$$\mathrm{OH^-} \rightleftharpoons \mathrm{Cl^-} \qquad K_{\mathrm{Cl-OH}} = K_{\mathrm{H+Cl}}/K_{\mathrm{w}} \tag{27}$$

where $k_{\mathrm{B}}T \ln K_{i-j} = (\mu_i - \mu_i^{\ominus}) - (\mu_j - \mu_j^{\ominus})$.

Both the set of particle exchange moves in Eq. 21 − Eq. 24 and the identity exchange moves in Eq. 26 and Eq. 27 are redundant. Therefore, a smaller subset of these moves is sufficient to exchange any ion pair through a chain of several exchange moves. In terms of the stoichiometric matrix formalism[93], the stoichiometric matrix of the exchange reactions must be of the same rank as the number of components. In Supporting Information, Section S6, we show several examples of sets of exchange moves that are not sufficient, and we discuss the resulting artefacts. A sufficient set of particle exchange moves can be realized by various combinations of the above examples. In addition to the minimal set of moves, some redundant combinations can also be included. Although they converge on the same final result, different moves may have different sampling efficiency under different conditions[94]. In theory, we could optimize the set of reactions on the fly by choosing the most abundant species under given conditions[95]. In practice, we should use a redundant set of reactions to obtain a robust combination of reactions in a broad range of pH values while adding only little computational overhead due to the redundant moves. Choosing a redundant set of moves is especially useful

when seeking to simulate a broad range of reservoir compositions, defined by the pH and ionic strength, because we can then employ same set of moves for all simulations. For example, the identity exchange moves in Eq. 26 and Eq. 22 are redundant with respect to ion pair insertions. However, they have a very low computational cost and can accelerate the simulation by efficiently improving the sampling.

Linking the reservoir chemical potentials, its composition and pH

In experiments, it is often convenient to specify the reservoir according to its composition, for example, by specifying the amount of NaCl that has been dissolved in water and the amount of NaOH or HCl that has been added to adjust the pH. Conversely, our simulation algorithm requires chemical potentials of the reservoir constituents as inputs. The relationship between the composition and the chemical potentials in a reservoir consisting of interacting particles is unique but complex. Therefore, we can either choose the chemical potentials and determine the reservoir composition in an auxiliary simulation, or we can choose the compositions, and determine the corresponding chemical potentials. Two additional constraints (the electroneutrality due to Eq. 25, and the value of K_{w}) imply that, in a reservoir with n constituents, only $(n-2)$ chemical potentials or concentrations can be chosen independently.

If we prefer to specify the reservoir by choosing the chemical potentials, we can choose two of the chemical potentials $\{\mu_{\mathrm{Na^+}}, \mu_{\mathrm{Cl^-}}, (\mu_{\mathrm{H^+}} \text{ or } \mu_{\mathrm{OH^-}})\}$, or equivalently two of the reaction constants $\{K_{\mathrm{Na+Cl}}, K_{\mathrm{H+Cl}}, K_{\mathrm{Na+OH}}\}$. The salt concentration in the reservoir then corresponds to the concentration of NaCl ion pairs, that is, $c^{\mathrm{res}}_{\mathrm{salt}} = \min\left(c^{\mathrm{res}}_{\mathrm{Na^+}}, c^{\mathrm{res}}_{\mathrm{Cl^-}}\right)$. The reservoir pH follows directly from $\mu_{\mathrm{H^+}}$. Depending on the pH, we can calculate the concentration of additional NaOH or HCl as $c_{\mathrm{NaOH}} = c^{\mathrm{res}}_{\mathrm{Na^+}} - c^{\mathrm{res}}_{\mathrm{salt}}$ or as $c_{\mathrm{HCl}} = c^{\mathrm{res}}_{\mathrm{Cl^-}} - c^{\mathrm{res}}_{\mathrm{salt}}$. This approach is termed herein **the calibration method**. If a specific value of $c^{\mathrm{res}}_{\mathrm{salt}}$ and a specific value of pH is desired, then the chemical potentials can be re-adjusted in an iterative procedure, starting from the ideal-gas chemical potentials as an initial guess. However, in such a case, it might be more convenient to use a different approach, as described in the

next paragraph.

If the reservoir is defined by its composition, then μ_i^{id} is known for all species, and μ_i^{ex} can be determined in an auxiliary simulation of the reservoir alone by **direct calculation of μ^{ex} using Widom particle insertion**[96]. In particular, the reservoir pH is not known a priori and must be calculated from the determined μ_{H^+}. Then, the difference $\mu_i - \mu_i^{\ominus} = \mu_i^{\mathrm{id}} + \mu_i^{\mathrm{ex}}$ can be computed, which is the required input parameter of the acceptance probability in Eq. 20. To ensure that the constraint $k_{\mathrm{B}}T \ln K_{\mathrm{w}} = \mu_{\mathrm{H}^+} + \mu_{\mathrm{OH}^-}$ is satisfied, the reservoir concentration of H^+ or OH^- should be adjusted iteratively, based on the calculated μ^{ex}. This is especially important if the reservoir ionic strength, I^{res}, is dominated by the H^+ or OH^- ions, that is, if $\mathrm{pH} \lesssim -\log_{10} c_{\mathrm{salt}}^{\mathrm{res}}/c^{\ominus}$, or $\mathrm{pOH} \lesssim -\log_{10} c_{\mathrm{salt}}^{\mathrm{res}}/c^{\ominus}$.

Neglecting the excess chemical potentials of ions in the reservoir and treating them as an ideal gas may cause up to 50% deviations between the actual reservoir concentration and the desired one. This estimate holds for 1:1 electrolytes at $c \approx 0.1\,\mathrm{M}$, and even stronger deviations occur if multivalent ions are present in the reservoir. Therefore, the excess chemical potential must be calculated for the specific model of ionic solution at a given reservoir composition. Furthermore, the simulation box used to determine the excess chemical potential should be large enough to accommodate at least 100 ion pairs at the given concentration in order to avoid problems with poor sampling[97]. Even if the concentration of some ion is low, (for example, the concentration of H^+ at $\mathrm{pH} \approx 7$), its excess chemical potential should be accounted for.

Computational Details

Parameters of the simulated systems

We simulated 16 polyelectrolyte chains, composed of $N = 50$ monomers per chain, in an implicit solvent and a cubic simulation box. We performed the simulations at different concentrations of monomer units, $c_{\mathrm{pol}} \in \{2.41, 0.435, 0.147, 0.067, 0.058\}\,\mathrm{M}$. The polyelectrolyte consisted of weak acidic monomers, with a given $\mathrm{p}K_{\mathrm{A}}$ value. The system was in equilibrium

with a reservoir corresponding to an aqueous solution of NaCl, whose pH was adjusted to the desired value by adding HCl or NaOH. We simulated the polyelectrolytes with various acidity constants, $\mathrm{p}K_\mathrm{A} \in \{1, 2, 3, 4\}$, in equilibrium with reservoirs at various pH values, $1 \leq \mathrm{pH} \leq 13$, and at various NaCl concentrations, $c_\mathrm{salt}^\mathrm{res} \in \{0.01, 0.02, 0.05, 0.1, 0.2\}\,\mathrm{M}$. We performed a set of auxiliary simulations of the reservoir with 400 ion pairs (Na^+ and Cl^-, 800 ions in total) to determine the chemical potentials of individual ionic species in the reservoir. Further technical details of the simulations are provided in Supporting Information, Section S1.

We used the reaction ensemble method to account for the ionization reaction. Because of the broad range of pH, H^+ and OH^- ions were often scarce in our simulations. Therefore, we implemented acid ionization reaction in Eq. 1 using reactions Eq. 16–Eq. 19. Na^+ and Cl^- ions were always present in sufficient number: thus, the acid protonation reaction was never affected by insufficient sampling. The system was coupled to the reservoir using the insertion of $\mathrm{Na}^+\mathrm{Cl}^-$ ion pairs, Eq. 21 and by identity exchange moves, Eq. 26 and 27. The G-RxMC method was implemented in the version 4.1 of the ESPResSo package, which we used for our simulations[98].

Computational Results

Donnan partitioning of ions

To validate our method of exchanging particles with the reservoir, we show that in the absence of interactions the ion partitioning follows the Donnan theory. We examine the Donnan partitioning in a three-component system in equilibrium with a two-component reservoir: the charged species A^-, which is present only in the system, and four different monovalent ions (two anions, two cations), which are exchanged between the system and the reservoir. To present partitioning of both coions and counterions on one master curve, we plot ξ_i for the coions (OH^- and Cl^-) and $(\xi_i - c_{\mathrm{A}^-}^\mathrm{sys}/I^\mathrm{res})$ for the counterions (H^+ and Na^+).

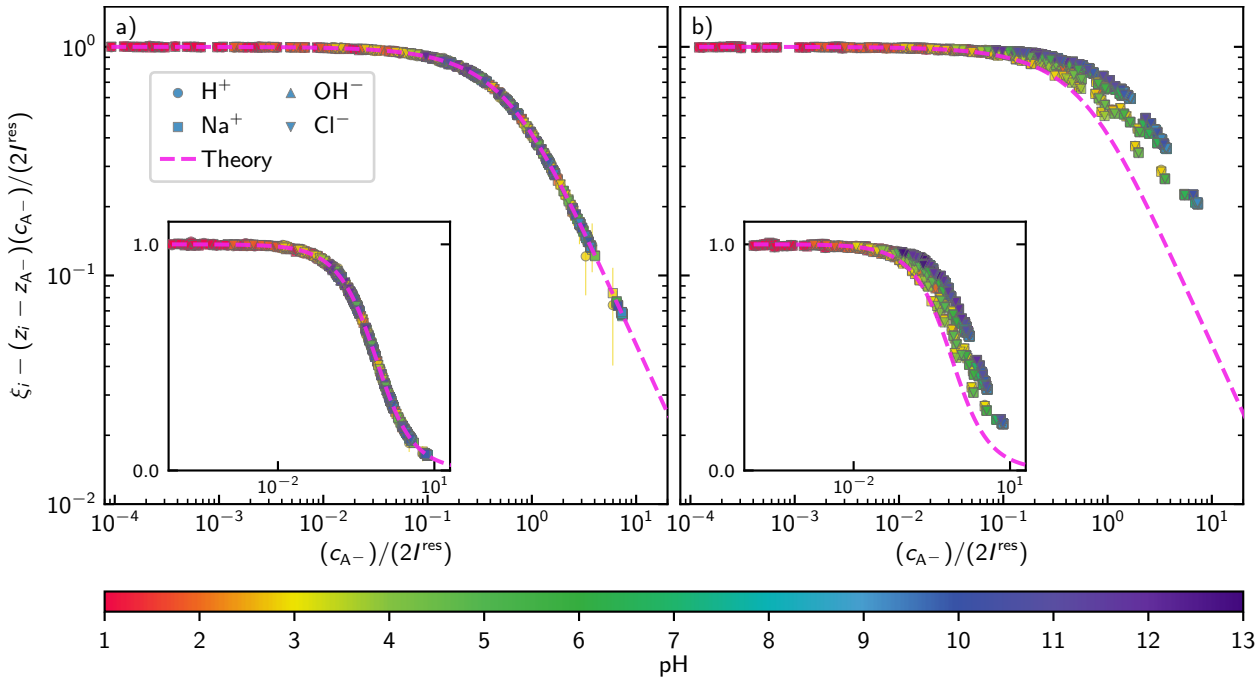

Figure 2: Comparison of ion partitioning predicted by the Donnan theory[85,87] with simulation results from the Grand-reaction method. The pink dashed line represents the generalized Donnan prediction. Partitioning of various ions from the simulations is encoded by different symbol shapes, as indicated in the legend. The color code indicates the reservoir pH in each simulation. Panel (a) shows the partitioning in an ideal system *without* interactions. Panel (b) shows the partitioning in a polymer solution *with* interactions. We omitted data points which correspond to fewer than 10 ions of a particular type in the simulation box because they are affected by poor sampling. A plot with these data points is provided in Supporting Information (Figure S1).

Both expressions dependent on $c^{\text{sys}}_{\text{A}^-}/2I^{\text{res}}$ and in an ideal system these expression are equal. We can combine both expressions as

$$\xi_i - (z_i - z_{\text{A}^-})c^{\text{sys}}_{\text{A}^-}/2I^{\text{res}} = \begin{cases} \xi_i, & \text{coions} \\ \xi_i - c^{\text{sys}}_{\text{A}^-}/I^{\text{res}}, & \text{counterions} \end{cases} \tag{28}$$

where z_i is the valency of ion i ($z_{\text{H}^+} = z_{\text{Na}^+} = +1$; $z_{\text{A}^-} = z_{\text{Cl}^-} = z_{\text{OH}^-} = -1$). For the counterions, we can interpret this expression as the partition coefficient, corrected by the number of ions neutralizing the polymer.

In Figure 2a, we show the ion partitioning from our simulations of a polyelectrolyte

solution in equilibrium with a multi-component reservoir, defined by the pH and by the amount of added salt. When switching off all interactions (Figure 2a), our implementation of particle exchange with the reservoir follows the Donnan partitioning (Eq. 28) in a broad range of pH values. When switching on interactions (Figure 2b), the partitioning of ions deviates from the Donnan prediction. All deviations shown in Figure 2b originate from intermolecular interactions. The cohesive effect of electrostatics causes positive deviations from the Donnan law, yielding higher concentrations of exchangeable ions in the system than those predicted by Eq. 28. This is consistent with experimental observations of ion partitioning in polyelectrolyte hydrogels[99] and with our simulations of these systems[38,78,79].

Ionization with Donnan partitioning: ideal vs. non-ideal system

To demonstrate the importance of coupling acid-base ionization with Donnan partitioning of ions, we examine its effect on the ionization degree. Similarly to the previous section, we first investigate the ideal system for which we can obtain exact analytical results as a reference. Without the Donnan partitioning, the ionization degree α(pH) follows the Henderson-Hasselbalch, Eq. 13 (denoted as HH in Fig.3a). By coupling the HH equation with the Donnan partitioning, Eq. 28, we obtain the results denoted as HH+Donnan. In Fig.3a, we show that the Grand-reaction method (G-RxMC) captures both effects correctly, it reproduces the HH+Donnan reference results. Under the given conditions, the Donnan effect decreases the ionization and shifts the titration curve to a higher pH value by ≈ 1 at $\alpha = 0.5$. We compare the above results with what we call the Grand-constant-pH (G-cpH) method, which resembles the G-RxMC method but treats the acid-base equilibrium using the cpH method instead of the RxMC method. Further details of the G-cpH method are given in Section S2 in Supporting Information. In contrast to the G-RxMC method, the G-cpH method reproduces the reference HH results without the Donnan partitioning, demonstrating that the cpH method fails to capture the Donnan contribution, even when the simulation includes ion exchange with the reservoir. Hence, the cpH method cannot be

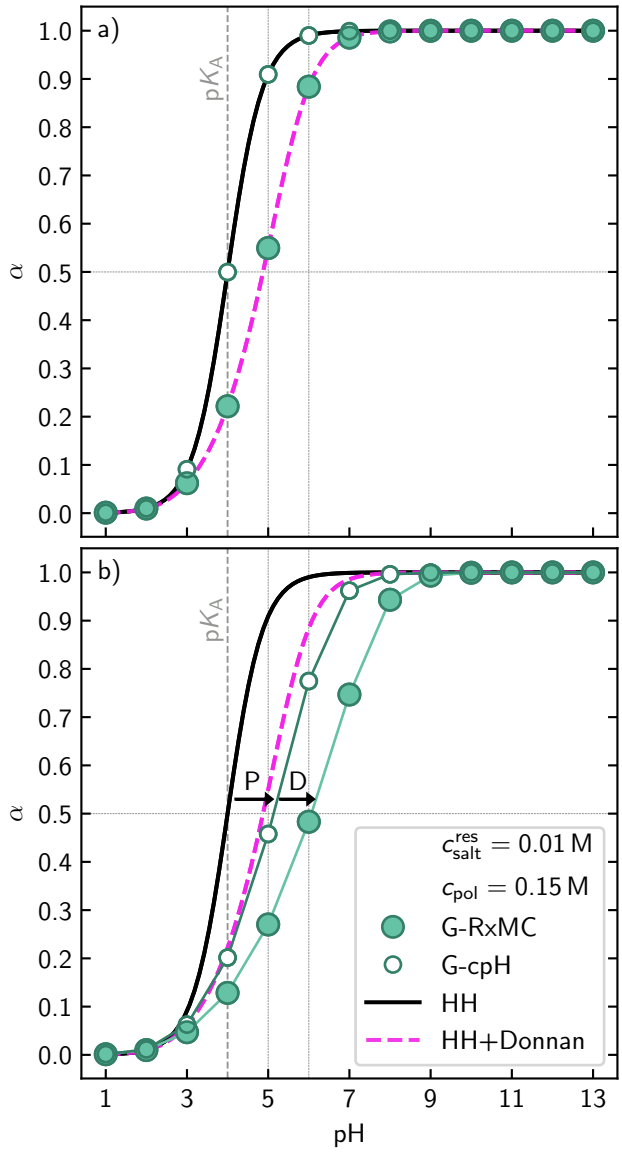

Figure 3: Ionization degree as a function of reservoir pH, comparing different methods. The top panel (a) shows an ideal system, while the bottom panel (b) shows an interacting system. Vertical and horizontal lines are guides to help estimating the magnitude of the Donnan and the polyelectrolyte effect at $\alpha = 0.5$. Arrows indicate the magnitude of the polyelectrolyte effect "P", and the Donnan effect "D".

used to simulate a system in equilibrium with a reservoir.

Interestingly, Fig 3b shows that a G-cpH simulation of the same system with interactions yields a shifted and deformed titration curve that almost coincides with the ideal results with the Donnan partitioning (HH+Donnan). However, the physical reasons for this shift are different: in the cpH simulation, it is caused predominantly by repulsion among the charges on the chain; in contrast, in the case of HH+Donnan, it is caused by different concentrations of H^+ ions in the system and in the reservoir. The former is the polyelectrolyte effect and the latter is the Donnan effect. Only the G-RxMC simulation captures both effects correctly, and yields a titration curve with a shift that is roughly the sum of the individual contributions. The magnitude of the Donnan effect in the interacting system can be estimated by considering the difference between the G-RxMC and G-cpH result. Similar to the non-interacting case, this estimate yields a shift of ≈ 1 on the pH scale at $\alpha = 0.5$, demonstrating that the shift in the titration curve due to the Donnan effect adds to the polyelectrolyte effect. This additivity follows from the fact that at a fixed I^{res} the Donnan potential depends mainly on the concentration of ionized groups in the system, which is uniquely determined by the ionization degree α.

We should consider limiting cases when either the polyelectrolyte effect or the Donnan effect dominates. According to Fig 2, the Donnan effect is strong when $c_{\text{A}^-} > 2I^{\text{res}}$. Therefore, this effect is particular important at high polymer concentrations or at low salinity of the reservoir. At polymer concentrations lower than I^{res}, the Donnan effect becomes small. Thus, the magnitude of the Donnan effect varies as a function of the polymer concentration, pH and reservoir salinity. The polyelectrolyte effect primarily depends on interactions between neighboring charges on the chain. These interactions are controlled by the charge density on the chain and by the electrostatic coupling, and they are strong for sufficiently long chains, $N \gtrsim 50$, and absent in short chains. For a given combination of a polyelectrolyte and a solvent, the polyelectrolyte effect increases with the ionization degree, qualitatively similarly to the Donnan effect. Therefore, one of these effects can be easily mistaken for

the other. As a rule of thumb, we can estimate that the polyelectrolyte effect will dominate at low polymer concentrations when the Donnan effect is weak even if the polymer is fully ionized. In turn, the Donnan effect will dominate when the fully ionized polymer has a low charge density but the polymer concentration in the system is sufficient to strengthen the Donnan effect. In many relevant situations, none of the limiting cases is applicable, and both effects may be of comparable magnitude. This complicated interplay between the polyelectrolyte effect and the Donnan partitioning makes it difficult to discern a priori, which of these effects is dominant, if any. Therefore, both of these effects must be correctly captured in simulations.

Effect of pH and ion partitioning on chain swelling

After assessing the Donnan effect and the polyelectrolyte effect on the ionization, we now examine how the salt and polymer concentrations affect the properties of weak polyelectrolytes under various conditions. We compare not only the degree of ionization but also the chain swelling, which can be directly determined in experiments. The variation of end-to-end distance as a function pH (Figure 4) shows that, unlike the ionization degree, chain swelling is affected by the reservoir pH on both ends of the pH scale. To differentiate the Donnan effect from the polyelectrolyte effect, we compare G-RxMC simulations (showing both the polyelectrolyte and the Donnan effect) with G-cpH simulations (showing only the polyelectrolyte effect). Both the polyelectrolyte effect and the Donnan effect suppress polymer ionization, shifting the titration curves to higher pH values (Figure 4a and c).

At a constant polymer concentration, $c_{\mathrm{pol}} = 0.06\mathrm{M}$ (Figure 4a), the Donnan effect and the polyelectrolyte effect both increase with the decrease in salt concentration. At $c_{\mathrm{salt}}^{\mathrm{res}} = 0.10\mathrm{M} \gtrsim c_{\mathrm{pol}}$, the small difference in the shift of G-cpH and G-RxMC curves indicates that the Donnan effect is weak, shifting the titration curve on the pH scale by ≈ 0.1. In contrast, the shift of both curves by ≈ 1 with respect to the Henderson-Hasselbalch (HH) curve indicates that the polyelectrolyte effect prevails. At $c_{\mathrm{salt}}^{\mathrm{res}} = 0.02\mathrm{M} \lesssim c_{\mathrm{pol}}$, the G-RxMC

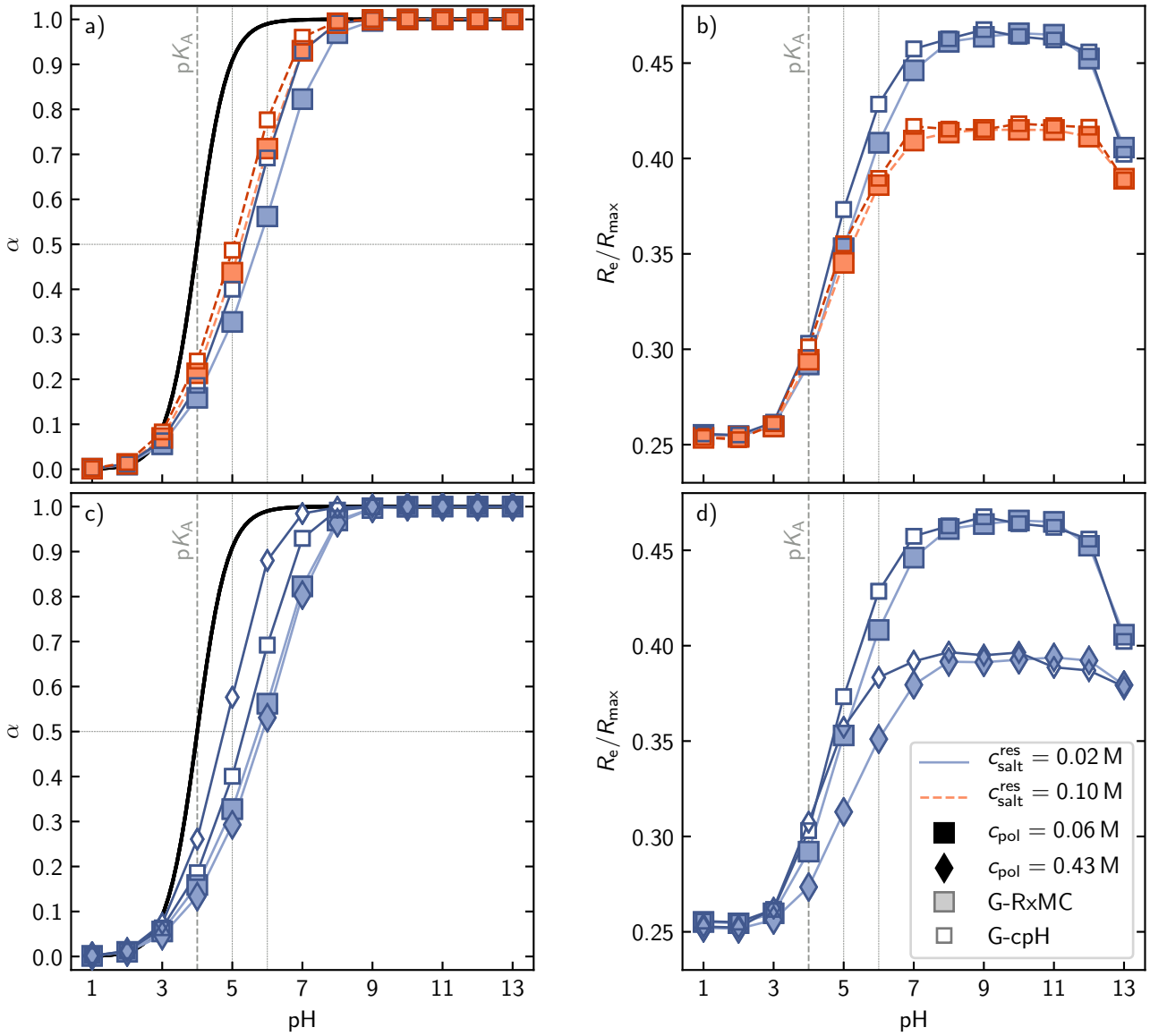

Figure 4: Degree of ionization (a + c) and end-to-end distance (b + d) of the weak polyelectrolyte chain with $pK_A = 4.0$ as a function of the reservoir pH. To differentiate the polyelectrolyte effect from the Donnan effect, we compare G-RxMC and G-cpH simulations. Salt concentrations in the reservoir and monomer concentrations are indicated in the legend. Error bars are on the order of the point size. Vertical and horizontal lines are guides to help estimating the magnitude of the Donnan and the polyelectrolyte effect at $\alpha = 0.5$.

curve is shifted to a higher pH by ≈ 0.5 further than the G-cpH curve, indicating that the Donnan effect is stronger; however, the polyelectrolyte effect still dominates the overall trend. The end-to-end distance of the chain, $R_{\mathrm{e}}(\mathrm{pH})$, (Fig. 4b) follows the same qualitative trend for both salt concentrations: an increase at pH $\approx \mathrm{p}K_{\mathrm{A}}$ caused by the increase in polymer ionization, followed by a plateau at $7 \lesssim \mathrm{pH} \lesssim 11$ when the polymer is fully ionized, and finally a de-swelling at pH $\gtrsim 12$ when the ionic strength is dominated by the OH^- ions. The system at a lower $c_{\mathrm{salt}}^{\mathrm{res}}$ exhibits a higher swelling in the plateau region because its ionic strength is lower.

At a constant salt concentration, $c_{\mathrm{salt}}^{\mathrm{res}} = 0.02\mathrm{M}$ (Figure 4c), the Donnan effect increases with the increase in the polymer concentration. However, the polyelectrolyte effect decreases with the increase in polymer concentration because the counterions of the polymer increase the ionic strength in the system. Therefore, the shift of the titration curve due to the polyelectrolyte effect in the G-cpH simulations at $c_{\mathrm{pol}} = 0.43\mathrm{M}$ is only ≈ 0.8 while at $c_{\mathrm{pol}} = 0.06\mathrm{M}$ it is ≈ 1.2. The combination of the Donnan effect and the polyelectrolyte effect in G-RxMC simulations yields almost identical shifts of $\alpha(\mathrm{pH})$ curves at both polymer concentrations in Figure 4c. The comparison of G-RxMC and G-cpH simulations in Figure 4c shows that, at lower polymer concentrations a rather weak Donnan effect (≈ 0.5 on the pH scale) is combined with a rather strong polyelectrolyte effect (≈ 1.2); In contrast, at higher polymer concentrations, both effects have similar magnitudes, shifting the curves by ≈ 0.8 on the pH scale. The end-to-end distance (Figure 4b and d) is a function of the degree of ionization and of the ionic strength in the system. Therefore, even though the $\alpha(\mathrm{pH})$ curves at constant salt concentration are nearly identical in Fig. 4c, they result in a mutually shifted swelling response, $R_{\mathrm{e}}(\mathrm{pH})$ in Fig. 4d. The magnitude of $R_{\mathrm{e}}(\mathrm{pH})$ is always higher at $c_{\mathrm{pol}} = 0.43\mathrm{M}$ because the ionic strength in the system at a given $\alpha(\mathrm{pH})$ increases with c_{pol}. Thus, when comparing the chain swelling at different polymer concentrations and at a fixed salt concentration, we observe a cancellation of the effects on the $\alpha(\mathrm{pH})$ curves but not on the $R_{\mathrm{e}}(\mathrm{pH})$ curves.

In general, this cancellation of effects, which we have demonstrated in special cases discussed in Fig. 4, is unexpected. Therefore, neglecting either the Donnan or the polyelectrolyte effect would lead to incorrect predictions. Furthermore, in Supporting Information, Section S9, we compare the G-RxMC simulations with simulations of a closed system, showing that Donnan partitioning cannot be neglected when simulating ionic polymers in equilibrium with a reservoir. Thus, both Donnan and polyelectrolyte effects must be captured to correctly predict α(pH) and R_{e}(pH) in a broad range of parameters.

The non-monotonic swelling as a function of pH and salt concentration, shown in Fig. 4, has been previously known from experiments and from numerical mean-field models; however, it has never been observed in coarse-grained simulations. Borisov et al.[100] predicted a non-monotonic swelling of star-like weak polyelectrolytes as a function of salt concentration and explained this effect by similar arguments: starting from low ionic strength, the stars first swell because their ionization degree increases with the ionic strength; at higher ionic strength, the fully ionized stars shrink because of ionic screening. A similar effect on the swelling of weak polyelectrolyte micelles was experimentally observed by Matějíček et al.[101]. Later, they confirmed this effect in simulations, combining explicit-particle representation of polymers with mean-field treatment of exchangeable ions on the Poisson-Boltzmann level[102]. The molecular theory of Longo et al.[82] also combined molecular representation of polyelectrolytes with mean-field treatment of exchangeable ions to observe a similar effect on the swelling of polyelectrolyte gels grafted to a surface. In the cases mentioned above, the mean-field representation of exchangeable ions made it possible to set the reservoir concentrations as boundary conditions. To our knowledge, our current results are the first demonstration of this effect in explicit-particle simulations.

Relation to previously published simulations

We compared our simulation method and our findings regarding the Donnan effect and the polyelectrolyte effect with similar methods and systems studied in literature. Rathee et

al.[60,61] published two articles where they investigated weak polyelectrolytes in equilibrium with two independent reservoirs; one consisting of a salt solution (NaCl or $MgSO_4$ at various concentrations) and the other consisting of KOH at $c = 10^{-2.7}\,\mathrm{M}$, to ensure a constant value of pH = 11.3. They varied the polymer ionization by varying the reaction constant of the ionization reaction. They formulated the acid-base reaction using Eq. 17, which allowed them to conveniently carry out simulations at pH > 11, and they mentioned that such a setup would become inefficient at lower pH values. Because they coupled the system to two independent reservoirs, they obtained different Donnan potentials and therefore different Donnan effects for the salt ions (Na^+Cl^-) and for the (K^+OH^-) ion pair. Consequently, the Donnan effect on the ionization reaction was controlled by the ionic strength in the KOH reservoir. We estimate that, in their first publication[61], the Donnan effect should be rather weak because the monomer concentrations were on the same order of magnitude as the ionic strength in the KOH bath. In addition, opposite charges on weak acids and bases in their system offset each other; further suppressing the Donnan effect. In their second publication[60], they employed a rather high concentration of ionizable monomers $c_{\mathrm{pol}} \approx 0.05\,\mathrm{M} \gg 10^{-\mathrm{pOH}}$. From the HH+Donnan model, we estimate a shift in their titration curve of ≈ 0.4 units of $\mathrm{p}K_\mathrm{A}$ due to the Donnan effect (see Supporting Information, Section S6). This shift significantly contributed to the observed overall shift in the titration curve (≈ 2.6 units of $\mathrm{p}K_\mathrm{A}$). However, they interpreted their results solely in terms of the polyelectrolyte effect and hydrophobic interactions, and they did not mention the Donnan effect.

In contrast to the simulation studies discussed in the previous paragraph, results from mean-field calculations of swelling of weak polyelectrolyte gels have been interpreted solely in terms of the Donnan effect, neglecting the polyelectrolyte effect. For example, Polotsky et al.[103] developed a mean-field model of weak polyelectrolyte gels, which accounted for the effect of Donnan partitioning on the ionization but completely neglected the polyelectrolyte effect. Therefore, their results[103] for polymer concentrations higher than salt concentrations remain valid because the Donnan effect should dominate, while their results for polymer

concentration lower than salt concentration should be revisited because the polyelectrolyte effect could dominate. In our recent publication[18], we used a numerical mean-field model that accounts for inter-particle interactions to model the swelling of weak polyelectrolyte gels in salt solutions as a function of reservoir pH. We have shown that the predicted shift in swelling and ionization of these gels as a function of $\mathrm{pH_{res}}$ can be quantified in terms of the local pH inside the gel ($\mathrm{pH_{sys}}$). In the current context, the difference ($\mathrm{pH_{sys}} - \mathrm{pH_{res}}$) is caused by the Donnan effect (cf. Eq.6 and Eq.13). After subtracting the Donnan effect, our results[18] suggest that the polyelectrolyte effect should cause a negative shift with respect to pH. Originally, we ascribed this negative shift to the inhomogeneous charge distribution within the gel. In the light of our current findings, we should ascribe this negative shift to artefacts of the spherically averaged mean-field representation that strongly underestimates the direct interaction between neighboring charges, which are the main cause of the polyelectrolyte effect.

The above account of published literature is by no means exhaustive. It should rather serve as a set of illustrative examples showing that various simulation and theoretical predictions for charge-regulating macromolecular systems in equilibrium with a reservoir should be revisited. Many such results have been interpreted in terms of either the Donnan effect or the polyelectrolyte effect but not both. Our current results show that, in some cases, such an approximation might be well justified, whereas it might lead to erroneous predictions in other cases.

Conclusion and outlook

In this study, we presented the Grand-reaction method (G-RxMC) for coarse-grained simulations of ionization equilibria coupled to a reservoir in a broad range of pH values. The pH and salt concentration are defined by the composition of the reservoir with which the system can exchange ions. Our method for simulating particle exchanges with the reservoir

and the ionization reaction naturally avoids known bottlenecks of previous simulations and nonphysical parameter combinations (pH and ionic strength) that can occur when using the constant-pH method. Our combination of particle exchanges enables efficient simulations also close to neutral pH, as long as the amount of added salt is not extremely low, $c_{\mathrm{salt}}^{\mathrm{res}} \gtrsim 10^{-4}\,\mathrm{M}$. A combination of neutral pH and low salt can still be simulated at moderate cost if finite-size effects are carefully considered. We will discuss this issue in full detail in a forthcoming publication. With the Grand-reaction method, the accessible pH range is no longer limited by the simulation algorithm. It is only limited by the applicability of the underlying model of ionic solution, as defined by the interaction potentials.

We demonstrated the importance of such a method by simulating a solution of weak polyelectrolytes as a model system. In the absence of interactions, our simulations reproduced the Donnan partitioning generalized to a multi-component reservoir. The Donnan effect due to ion partitioning decreases the pH in the system, and decreases ionization of the weak polyacid that cannot be exchanged between the reservoir and the system. In the presence of interactions, deviations from the ideal Donnan partitioning can be explained by charge-charge correlations. Charge-charge repulsion also leads to a shift in titration curves that is known for weak polyelectrolytes in solutions and termed as the polyelectrolyte effect. The titration curve of a polyelectrolyte solution in equilibrium with a reservoir is affected by both, Donnan effect and polyelectrolyte effect, and these effects depend on different parameters. The Donnan effect depends on the ratio of polymer concentration and ionic strength in the reservoir, whereas the polyelectrolyte effect depends on the separation of charges on the polymer chain and on the ionic strength in the system. Both effects shift the titration curve $\alpha(\mathrm{pH})$ to higher pH values. In special cases, both effects can lead to almost identical results, although for different physical reasons. In some limiting cases, one effect prevails, whereas the other one is negligible. In general, their overall influence is additive. Therefore neglecting one or the other might lead to erroneous conclusions. At $\mathrm{pH} \gtrsim \mathrm{p}K_{\mathrm{A}}$, the swelling of polyelectrolytes is affected by both effects similarly to the titration curves. In addition,

the swelling is affected by the Donnan effect also at pH $\gg$ pK_{A}, when the polyelectrolyte is fully ionized. By confronting selected published results we showed that it might be necessary to revisit some observations that have been interpreted solely in terms of the Donnan or the polyelectrolyte effect.

The presented method and simulation protocols can be generalized beyond our example system of a polyelectrolyte solution. The method can be used for any macromolecular or colloidal system in equilibrium with a reservoir at a given pH and salt concentration. The same principles and guidelines can be applied to simulate systems with weak polyelectrolyte gels in a reservoir or attached to a surface, interpolyelectrolyte complexes in equilibrium with a reservoir solution, peptides or proteins in salt solutions. In such systems, the effect of pH and salt on ionization is routinely exploited in experiments, and the observations are often interpreted assuming ideal ionization response. Our method enables us to predict the properties of such systems from computer simulations previously unavailable in the literature.

Extensions of the Grand-reaction method to a reservoir with more components, or to multiple chemical reactions in the system, are straightforward. Another extension of our method is a more sophisticated treatment of ions, such that they do not have identical parameters. We can account for the different effective radii of the hydrated ions[104], which affects their excess chemical potential. The influence of multivalent ions could also be simulated using this approach. In both cases, the calculation of reservoir chemical potentials would need to be modified because different interaction parameters imply different excess chemical potentials of each ion. In such cases, the calibration method might be more suitable to determine the reservoir chemical potentials. Finally, we point out that the Grand-reaction method is not suitable for simulating a bulk solution of weak polyelectrolytes at a given pH. For such a system we recommend using the constant-pH method[43] with an ionic strength matched to the buffer composition at the desired pH. Conversely, the Grand-reaction method should be used for simulating any system where partitioning of ions between two phases is relevant.

Acknowledgments

PK, PH, OR and RL acknowledge the financial support of the Czech Science foundation, grant 17-02411Y. RL and PK additionally acknowledge the support from the Grant agency of the Charles University, GAUK 978218. CH and JL thank the funding from the German Research Foundation (DFG) - 423435431 as part of FOR2811 and from the DFG through Grants HO 1108/26-1 and AR 593/7-1.

Supporting Information Available

The following files are available free of charge.

- esi.pdf contains descriptions of the following topics:
  - the Donnan partitioning
  - the exclusion radius used during the simulation
  - the required set of particle insertions
  - the measured excess chemical potential
  - the degree of ionization as a function of pH

References

(1) Crespo, J. G., Böddeker, K. W., Eds. *Membrane Processes in Separation and Purification*; Springer Netherlands: Dordrecht, 1994; DOI: 10.1007/978-94-015-8340-4.

(2) van Lente, J. J.; Claessens, M. M. A. E.; Lindhoud, S. Charge-Based Separation of Proteins Using Polyelectrolyte Complexes as Models for Membraneless Organelles. *Biomacromolecules* **2019**, *20*, 3696–3703, DOI: 10.1021/acs.biomac.9b00701.

(3) Tasker, J. B. Clinical Osmometry in Veterinary Medicine. *Bulletin of the American Society of Veterinary Clinical Pathologists* **1975**, *4*, 3–13, DOI: 10.1111/j.1939-165X.1975.tb00911.x.

(4) Rose, B. D. *Clinical Physiology of Acid-Base Disorders.*; Mcgraw-Hill: Place of publication not identified, 2011; OCLC: 704062347.

(5) Daugirdas, J. T.; Blake, P. G.; Ing, T. S. *Handbook of Dialysis*; Wolters Kluwer Health: S.l., 2014; OCLC: 1105388949.

(6) Mulder, M. *Basic Principles of Membrane Technology*; 1996; OCLC: 1105291754.

(7) Shannon, M. A.; Bohn, P. W.; Elimelech, M.; Georgiadis, J. G.; Mariñas, B. J.; Mayes, A. M. Science and Technology for Water Purification in the Coming Decades. *Nature* **2008**, *452*, 301–310, DOI: 10.1038/nature06599.

(8) Kucera, J. In *Kirk-Othmer Encyclopedia of Chemical Technology*; Inc, J. W. . S., Ed.; John Wiley & Sons, Inc.: Hoboken, NJ, USA, 2017; pp 1–44, DOI: 10.1002/0471238961.1805220502080120.a01.pub3.

(9) Gotoh, T.; Sano, M.; Nakai, S. Selective Recovery of Metal Ion by Using Hydrogel With Different Inner pH. *Macromolecular Symposia* **2019**, *385*, 1800163, DOI: 10.1002/masy.201800163.

(10) Klaus Opwis, J. S. G., Thomas Mayer-Gall Recovery of Noble Metals by the Use of Functional Adsorber Textiles. *Tekstil* **2016**, *65*, 322–326.

(11) Arens, L.; Weißenfeld, F.; Klein, C. O.; Schlag, K.; Wilhelm, M. Osmotic engine: Translating osmotic pressure into macroscopic mechanical force via poly (acrylic acid) based hydrogels. *Advanced Science* **2017**, *4*, 1700112.

(12) van Rijssel, J.; Costo, R.; Vrij, A.; Philipse, A. P.; Erné, B. H. Thermodynamic Charge-to-Mass Sensor for Colloids, Proteins, and Polyelectrolytes. *ACS Sensors* **2016**, *1*, 1344–1350, DOI: 10.1021/acssensors.6b00510.

(13) Chang, L.-W.; Lytle, T. K.; Radhakrishna, M.; Madinya, J. J.; Vélez, J.; Sing, C. E.; Perry, S. L. Sequence and entropy-based control of complex coacervates. *Nature Communications* **2017**, *8*, DOI: 10.1038/s41467-017-01249-1.

(14) Zhang, P.; Shen, K.; Alsaifi, N. M.; Wang, Z.-G. Salt Partitioning in Complex Coacervation of Symmetric Polyelectrolytes. *Macromolecules* **2018**, *51*, 5586–5593, DOI: 10.1021/acs.macromol.8b00726.

(15) Danielsen, S. P. O.; McCarty, J.; Shea, J.-E.; Delaney, K. T.; Fredrickson, G. H. Small ion effects on self-coacervation phenomena in block polyampholytes. *The Journal of Chemical Physics* **2019**, *151*, 034904, DOI: 10.1063/1.5109045.

(16) Li, L.; Srivastava, S.; Andreev, M.; Marciel, A. B.; de Pablo, J. J.; Tirrell, M. V. Phase Behavior and Salt Partitioning in Polyelectrolyte Complex Coacervates. *Macromolecules* **2018**, *51*, 2988–2995, DOI: 10.1021/acs.macromol.8b00238.

(17) Borisov, O. V.; Zhulina, E. B.; Leermakers, F. A.; Ballauff, M.; Müller, A. H. E. In *Self Organized Nanostructures of Amphiphilic Block Copolymers I*; Müller, A. H. E., Borisov, O., Eds.; Adv. Polym. Sci.; Springer Berlin Heidelberg, 2011; Vol. 241; pp 1–55.

(18) Rud, O.; Richter, T.; Borisov, O.; Holm, C.; Košovan, P. A self-consistent mean-field model for polyelectrolyte gels. *Soft Matter* **2017**, *13*, 3264–3274, DOI: 10.1039/C6SM02825J.

(19) Arnold, R. The titration of polymeric acids. *Journal of Colloid Science* **1957**, *12*, 549–556, DOI: 10.1016/0095-8522(57)90060-0.

(20) Jönsson, B.; Ullner, M.; Peterson, C.; Sommelius, O.; Södeberg, B. Titrating Polyelectrolytes – Variational Calculations and Monte Carlo Simulations. *Journal of Physical Chemistry* **1996**, *100*, 409–417.

(21) Ullner, M.; Woodward, C. E. Simulations of the titration of linear polyelectrolytes with explicit simple ions: Comparisons with screened Coulomb models and experiments. *Macromolecules* **2000**, *33*, 7144–7156.

(22) Ullner, M.; Jönsson, B.; Söderberg, B.; Peterson, C. A Monte Carlo study of titrating polyelectrolytes. *The Journal of Chemical Physics* **1996**, *104*, 3048–3057, DOI: http://dx.doi.org/10.1063/1.471071.

(23) Ullner, M.; Jönsson, B. A Monte Carlo Study of Titrating Polyelectrolytes in the Presence of Salt. *Macromolecules* **1996**, *29*, 6645–6655, DOI: 10.1021/ma960309w.

(24) Nová, L.; Uhlík, F.; Košovan, P. Local pH and effective pKA of weak polyelectrolytes – insights from computer simulations. *Physical Chemistry Chemical Physics* **2017**, *19*, 14376–14387, DOI: 10.1039/c7cp00265c.

(25) Murmiliuk, A.; Košovan, P.; Janata, M.; Procházka, K.; Uhlík, F.; Štěpánek, M. Local pH and Effective p K of a Polyelectrolyte Chain: Two Names for One Quantity? *ACS Macro Letters* **2018**, *7*, 1243–1247, DOI: 10.1021/acsmacrolett.8b00484.

(26) Lund, M.; Jönsson, B. On the Charge Regulation of Proteins. *Biochemistry* **2005**, *44*, 5722–5727, DOI: 10.1021/bi047630o.

(27) Lund, M.; Jönsson, B. Charge regulation in biomolecular solution. *Quarterly reviews of biophysics* **2013**, *46*, 265–281.

(28) Markovich, T.; Andelman, D.; Podgornik, R. Complex fluids with mobile charge-regulating macro-ions. *EPL (Europhysics Letters)* **2018**, *120*, 26001.

(29) Avni, Y.; Markovich, T.; Podgornik, R.; Andelman, D. Charge regulating macro-ions in salt solutions: screening properties and electrostatic interactions. *Soft matter* **2018**, *14*, 6058–6069.

(30) Frenkel, D.; Smit, B. *Understanding Molecular Simulation*, 2nd ed.; Academic Press: San Diego, 2002; DOI: 10.1016/B978-0-12-267351-1.X5000-7.

(31) Valleau, J. P.; Cohen, L. K. Primitive model electrolytes. I. Grand canonical Monte Carlo computations. *The Journal of Chemical Physics* **1980**, *72*, 5935–5941, DOI: 10.1063/1.439092.

(32) Carrillo, J.-M. Y.; Dobrynin, A. V. Polyelectrolytes in Salt Solutions: Molecular Dynamics Simulations. *Macromolecules* **2011**, *44*, 5798–5816, DOI: 10.1021/ma2007943.

(33) Barr, S. A.; Panagiotopoulos, A. Z. Grand-canonical Monte Carlo method for Donnan equilibria. *Physical Review E* **2012**, *86*, DOI: 10.1103/physreve.86.016703.

(34) Chang, R.; Kim, Y.; Yethiraj, A. Osmotic Pressure of Polyelectrolyte Solutions with Salt: Grand Canonical Monte Carlo Simulation Studies. *Macromolecules* **2015**, *48*, 7370–7377, DOI: 10.1021/acs.macromol.5b01610.

(35) Edgecombe, S.; Schneider, S.; Linse, P. Monte Carlo Simulations of Defect-Free Cross-Linked Gels in the Presence of Salt. *Macromolecules* **2004**, *37*, 10089–10100, DOI: 10.1021/ma0486391.

(36) Yin, D.-W.; de la Cruz, M. O.; de Pablo, J. J. Swelling and collapse of polyelectrolyte gels in equilibrium with monovalent and divalent electrolyte solutions. *Journal of Chemical Physics* **2009**, *131*, 194907–6.

(37) Carrillo, J.-M. Y.; Dobrynin, A. V. Salt Effect on Osmotic Pressure of Polyelectrolyte Solutions: Simulation Study. *Polymers* **2014**, *6*, 1897–1913, DOI: 10.3390/polym6071897.

(38) Košovan, P.; Richter, T.; Holm, C. Modeling of Polyelectrolyte Gels in Equilibrium with Salt Solutions. *Macromolecules* **2015**, *48*, 7698–7708, DOI: 10.1021/acs.macromol.5b01428.

(39) Höpfner, J.; Richter, T.; Košovan, P.; Holm, C.; Wilhelm, M. In *Intelligent Hydrogels*; Sadowski, G., Richtering, W., Eds.; Progress in Colloid and Polymer Science; Springer International Publishing, 2013; Vol. 140; pp 247–263, DOI: 10.1007/978-3-319-01683-2_19.

(40) Smith, E. R. Calculating the pressure in simulations using periodic boundary conditions. *Journal of Statistical Physics* **1994**, *77*, 449–472.

(41) Johnson, J. K.; Panagiotopoulos, A. Z.; Gubbins, K. E. Reactive canonical Monte Carlo: a new simulation technique for reacting or associating fluids. *Molecular Physics* **1994**, *81*, 717–733.

(42) Heath Turner, C.; Brennan, J. K.; Lisal, M.; Smith, W. R.; Karl Johnson, J.; Gubbins, K. E. Simulation of chemical reaction equilibria by the reaction ensemble Monte Carlo method: a review. *Molecular Simulation* **2008**, *34*, 119–146.

(43) Reed, C. E.; Reed, W. F. Monte Carlo study of titration of linear polyelectrolytes. *Journal of Chemical Physics* **1992**, *96*, 1609.

(44) Uhlík, F.; Košovan, P.; Limpouchová, Z.; Procházka, K.; Borisov, O. V.; Leermakers, F. A. M. Modeling of Ionization and Conformations of Starlike Weak Polyelectrolytes. *Macromolecules* **2014**, *47*, 4004–4016, DOI: 10.1021/ma500377y.

(45) Uhlík, F.; Košovan, P.; Zhulina, E. B.; Borisov, O. V. Charge-controlled nanostructuring in partially collapsed star-shaped macromolecules. *Soft Matter* **2016**, 4846–4852, DOI: 10.1039/c6sm00109b.

(46) Fernandez-Alvarez, R.; Nová, L.; Uhlík, F.; Kereïche, S.; Uchman, M.; Košovan, P.; Matějíček, P. Interactions of star-like polyelectrolyte micelles with hydrophobic counterions. *Journal of Colloid and Interface Science* **2019**, *546*, 371 – 380, DOI: https://doi.org/10.1016/j.jcis.2019.03.054.

(47) Sean, D.; Landsgesell, J.; Holm, C. Computer Simulations of Static and Dynamical Properties of Weak Polyelectrolyte Nanogels in Salty Solutions. *Gels* **2018**, *4*, 2, DOI: 10.3390/gels4010002.

(48) Sean, D.; Landsgesell, J.; Holm, C. Influence of weak groups on polyelectrolyte mobilities. *Electrophoresis* **2019**, *40*, 799–809, DOI: 10.1002/elps.201800346.

(49) Ullner, M.; Jönsson, B.; Widmark, P. O. Polyelectrolytes - Monte-Carlo Simulation And Scaling Arguments. *Journal of Chemical Physics* **1994**, *100*, 3365–3366.

(50) Ullner, M.; Jönsson, B.; Soderberg, B.; Peterson, C. A Monte Carlo study of titrating polyelectrolytes. *Journal of Chemical Physics* **1996**, *104*, 3048–3057.

(51) Ullner, M.; Jönsson, B. A Monte Carlo study of titrating polyelectrolytes in the presence of salt. *Macromolecules* **1996**, *29*, 6645–6655.

(52) Ullner, M.; Woodward, C. E. Simulations of the titration of linear polyelectrolytes with explicit simple ions: Comparisons with screened Coulomb models and experiments. *Macromolecules* **2000**, *33*, 7144–7156.

(53) Carnal, F.; Ulrich, S.; Stoll, S. Influence of explicit ions on titration curves and conformations of flexible polyelectrolytes: A Monte Carlo study. *Macromolecules* **2010**, *43*, 2544–2553, DOI: 10.1021/ma901909b.

(54) Carnal, F.; Stoll, S. Adsorption of weak polyelectrolytes on charged nanoparticles. Impact of salt valency, pH, and nanoparticle charge density. Monte Carlo simulations. *The Journal of Physical Chemistry B* **2011**, *115*, 12007–12018.

(55) Stornes, M.; Linse, P.; Dias, R. S. Monte Carlo Simulations of Complexation between Weak Polyelectrolytes and a Charged Nanoparticle. Influence of Polyelectrolyte Chain Length and Concentration. *Macromolecules* **2017**, *50*, 5978–5988, DOI: 10.1021/acs.macromol.7b00844.

(56) Stornes, M.; Shrestha, B.; Dias, R. S. pH-Dependent Polyelectrolyte Bridging of Charged Nanoparticles. *J. Phys. Chem. B* **2018**, *122*, 10237–10246, DOI: 10.1021/acs.jpcb.8b06971.

(57) Hofzumahaus, C.; Hebbeker, P.; Schneider, S. Monte Carlo simulations of weak polyelectrolyte microgels: pH-dependence of conformation and ionization. *Soft Matter* **2018**, *14*, 4087–4100.

(58) Landsgesell, J.; Nova, L.; Rud, O.; Uhlik, F.; Sean, D.; Hebbeker, P.; Holm, C.; Košovan, P. Simulations of ionization equilibria in weak polyelectrolyte solutions and gels. *Soft Matter* **2019**, *15*, 1155–1185, DOI: 10.1039/C8SM02085J.

(59) Landsgesell, J.; Holm, C.; Smiatek, J. Simulation of weak polyelectrolytes: A comparison between the constant pH and the reaction ensemble method. *The European Physical Journal Special Topics* **2017**, *226*, 725–736, DOI: 10.1140/epjst/e2016-60324-3.

(60) Rathee, V.; Sidky, H.; Sikora, B.; Whitmer, J. Explicit Ion Effects on the Charge and Conformation of Weak Polyelectrolytes. *Polymers* **2019**, *11*, 183, DOI: 10.3390/polym11010183.

(61) Rathee, V. S.; Sidky, H.; Sikora, B. J.; Whitmer, J. K. Role of Associative Charging in the Entropy–Energy Balance of Polyelectrolyte Complexes. *Journal of the American Chemical Society* **2018**, *140*, 15319–15328, DOI: 10.1021/jacs.8b08649.

(62) Hill, T. L. Thermodynamics of Small Systems. *Journal of Chemical Physics* **1962**, *36*, 3182–3197.

(63) Moreira, A. G.; Netz, R. R. In *Electrostatic Effects in Soft Matter and Biophysics*; Holm, C., Kékicheff, P., Podgornik, R., Eds.; NATO Science Series II - Mathematics, Physics and Chemistry; Kluwer Academic Publishers: Dordrecht, Nl, 2001; Vol. 46.

(64) Biesheuvel, P. M.; Leermakers, F. A. M.; Cohen Stuart, M. A. Self-consistent field theory of protein adsorption in a non-Gaussian polyelectrolyte brush. *Physical Review E: Statistical, Nonlinear, and Soft Matter Physics* **2006**, *73*, 011802, DOI: 10.1103/PhysRevE.73.011802.

(65) Biesheuvel, P. M.; Mauser, T.; Sukhorukov, G. B.; Mohwald, H. Micromechanical Theory for pH-Dependent Polyelectrolyte Multilayer Capsule Swelling. *Macromolecules* **2006**, *39*, 8480–8486, DOI: 10.1021/ma061350u.

(66) Klein Wolterink, J.; van Male, J.; Cohen Stuart, M. A.; Koopal, L. K.; Zhulina, E. B.; Borisov, O. V. Annealed Star-branched Polyelectrolytes in Solution. *Macromolecules* **2002**, *35*, 9176–9190.

(67) Leermakers, F. A. M.; Ballauff, M.; Borisov, O. V. Counterion Localization in Solutions of Starlike Polyelectrolytes and Colloidal Polyelectrolyte Brushes: A Self-Consistent Field Theory. *Langmuir* **2008**, *24*, 10026–10034, DOI: 10.1021/la8013249.

(68) Israëls, R.; Leermakers, F. A. M.; Fleer, G. J. On the Theory of Grafted Weak Polyacids. *Macromolecules* **1994**, *27*, 3087–3093, DOI: 10.1021/ma00089a028.

(69) Longo, G. S.; de la Cruz, M. O.; Szleifer, I. Molecular Theory of Weak Polyelectrolyte Gels: The Role of pH and Salt Concentration. *Macromolecules* **2011**, *44*, 147–158.

(70) Nap, R. J.; Park, S. H.; Szleifer, I. Competitive calcium ion binding to end-tethered weak polyelectrolytes. *Soft Matter* **2018**, *14*, 2365–2378, DOI: 10.1039/c7sm02434g.

(71) Barroso daSilva, F. L.; Dias, L. G. Development of constant-pH simulation methods in implicit solvent and applications in biomolecular systems. *Biophysical Reviews* **2017**, *9*, 699–728, DOI: 10.1007/s12551-017-0311-5.

(72) Rud, O. V.; Mercurieva, A. A.; Leermakers, F. A. M.; Birshtein, T. M. Collapse of Polyelectrolyte Star. Theory and Modeling. *Macromolecules* **2012**, *45*, 2145–2160, DOI: 10.1021/ma202201m.

(73) Klein Wolterink, J.; van Male, J.; Daoud, M.; Borisov, O. V. Starburst polyelectrolytes: Scaling and self-consistent-field theory. *Macromolecules* **2003**, *36*, 6624–6631.

(74) Israëls, R.; Leermakers, F. A. M.; Fleer, G. J.; Zhulina, E. B. Charged Polymeric Brushes: Structure and Scaling Relations. *Macromolecules* **1994**, *27*, 3249–3261, DOI: 10.1021/ma00090a018.

(75) Leermakers, F. A. M.; Ballauff, M.; Borisov, O. V. On the mechanism of uptake of globular proteins by polyelectrolyte brushes: A two-gradient self-consistent field analysis. *Langmuir* **2007**, *23*, 3937–3946, DOI: 10.1021/la0632777.

(76) Nap, R. J.; Tagliazucchi, M.; Szleifer, I. Born energy, acid-base equilibrium, structure and interactions of end-grafted weak polyelectrolyte layers. *The Journal of Chemical Physics* **2014**, *140*, 024910, DOI: 10.1063/1.4861048.

(77) Longo, G. S.; de la Cruz, M. O.; Szleifer, I. Molecular theory of weak polyelectrolyte thin films. *Soft Matter* **2012**, *8*, 1344–1354.

(78) Landsgesell, J.; Sean, D.; Kreissl, P.; Szuttor, K.; Holm, C. Modeling Gel Swelling Equilibrium in the Mean Field: From Explicit to Poisson-Boltzmann Models. *Physical Review Letters* **2019**, *122*, 208002, DOI: 10.1103/PhysRevLett.122.208002.

(79) Landsgesell, J.; Holm, C. Cell Model Approaches for Predicting the Swelling and

Mechanical Properties of Polyelectrolyte Gels. *Macromolecules* **2019**, *52*, 9341–9353, DOI: 10.1021/acs.macromol.9b01216.

(80) Nap, R. J.; Tagliazucchi, M.; Gonzalez Solveyra, E.; Ren, C.-l.; Uline, M. J.; Szleifer, I. *Polymer and Biopolymer Brushes*; Wiley-Blackwell, 2017; Chapter 6, pp 161–221, DOI: 10.1002/9781119455042.ch6.

(81) Tagliazucchi, M.; Calvo, E. J.; Szleifer, I. Molecular modeling of responsive polymer films. *AIChE Journal* **2010**, *56*, 1952–1959.

(82) Longo, G. S.; de la Cruz, M. O.; Szleifer, I. Non-monotonic swelling of surface grafted hydrogels induced by pH and/or salt concentration. *The Journal of Chemical Physics* **2014**, *141*, 124909, DOI: 10.1063/1.4896562.

(83) Longo, G. S.; de la Cruz, M. O.; Szleifer, I. pH-Controlled Nanoaggregation in Amphiphilic Polymer Co-networks. *ACS Nano* **2013**, *7*, 2693–2704, DOI: 10.1021/nn400130c.

(84) Uhlík, F.; Limpouchová, Z.; Jelínek, K.; Procházka, K. Polyelectrolyte shells of copolymer micelles in aqueous solutions: A Monte Carlo study. *Journal of Chemical Physics* **2004**, *121*, 2367–2375, DOI: 10.1063/1.1763571.

(85) Donnan, F. G. The Theory of Membrane Equilibria. *Chemical Reviews* **1924**, *1*, 73–90, DOI: 10.1021/cr60001a003.

(86) Ricka, J.; Tanaka, T. Swelling of ionic gels: quantitative performance of the Donnan theory. *Macromolecules* **1984**, *17*, 2916–2921, DOI: 10.1021/ma00142a081.

(87) Philipse, A.; Vrij, A. The Donnan equilibrium: I. On the thermodynamic foundation of the Donnan equation of state. *Journal of Physics: Condensed Matter* **2011**, *23*, 194106.

(88) Ewing, M.; Lilley, T.; Olofsson, G.; Ratzsch, M.; Somsen, G. Standard quantities in chemical thermodynamics. Fugacities, activities and equilibrium constants for pure and mixed phases (IUPAC Recommendations 1994). *Pure and Applied Chemistry* **1994**, *66*, 533–552.

(89) Buck, R. P.; Rondinini, S.; Covington, A. K.; Baucke, F. G. K.; Brett, C. M. A.; Camoes, M. F.; Milton, M. J. T.; Mussini, R.; Naumann, R.; Pratt, K. W.; Spitzer, P.; Wilson, G. S. Measurement of pH. Definition, standards, and procedures (IUPAC Recommendations 2002). *Pure and Applied Chemistry* **2002**, *74*, 2169.

(90) McNaught,; Wilkinson, *IUPAC. Compendium of Chemical Terminology, 2nd ed. (the "Gold Book")*; 1997; DOI: 10.1351/goldbook.

(91) van Male, J. Self-consistent-field theory for chain molecules: extensions, computational aspects, and applications. Ph.D. thesis, Wageningen University, 2003.

(92) Valleau, J. P.; Cohen, L. K. Primitive model electrolytes. I. Grand canonical Monte Carlo computations. *The Journal of Chemical Physics* **1980**, *72*, 5935–5941, DOI: 10.1063/1.439092.

(93) Smith, W. R.; Missen, R. W. What Is Chemical Stoichiometry?. *Chemical Engineering Education* **1979**, *13*, 26–32.

(94) Carrero-Mantilla, J.; Llano-Restrepo, M. Chemical equilibria of multiple-reaction systems from reaction ensemble Monte Carlo simulation and a predictive equation of state: combined hydrogenation of ethylene and propylene. *Fluid phase equilibria* **2006**, *242*, 189–203.

(95) Smith, W. R.; Missen, R. W. *Chemical Reaction Equilibrium Analysis: Theory and Algorithms*, reprint ed., with corrections ed.; Krieger: Malabar, Fla, 1991.

(96) Frenkel, D. Colloidal systems: Playing Tricks with Designer "Atoms". *Science* **2002**, *296*, 65.

(97) Smit, B.; Frenkel, D. An explicit expression for finite-size corrections to the chemical potential. *Journal of Physics: Condensed Matter* **1989**, *1*, 8659.

(98) Weik, F.; Weeber, R.; Szuttor, K.; Breitsprecher, K.; de Graaf, J.; Kuron, M.; Landsgesell, J.; Menke, H.; Sean, D.; Holm, C. ESPResSo 4.0 – an extensible software package for simulating soft matter systems. *The European Physical Journal Special Topics* **2019**, *227*, 1789–1816, DOI: 10.1140/epjst/e2019-800186-9.

(99) Katchalsky, A.; Michaeli, I. Polyelectrolyte gels in salt solutions. *Journal of Polymer Science* **1955**, *15*, 69.

(100) Borisov, O. V.; Zhulina, E. B.; Leermakers, F. A.; Ballauff, M.; Müller, A. H. E. In *Self Organized Nanostructures of Amphiphilic Block Copolymers I*; Müller, A. H. E., Borisov, O., Eds.; Adv. Polym. Sci.; Springer Berlin / Heidelberg, 2011; Vol. 241; pp 1–55, DOI: 10.1007/12_2010_104.

(101) Matějicek, P.; Podhajecka, K.; Humpolicková, J.; Uhlik, F.; Jelinek, K.; Limpouchova, Z.; Prochazka, K.; Špirková, M. Polyelectrolyte behavior of polystyrene-block-poly (methacrylic acid) micelles in aqueous solutions at low ionic strength. *Macromolecules* **2004**, *37*, 10141–10154.

(102) Matějiček, P.; Uchman, M.; Lokajová, J.; Štěpánek, M.; Špirková, M.; Procházka, K. Multilayer Polymeric Nanoparticles Based on Specific Interactions in Solution: Polystyrene-block-poly (methacrylic acid) Micelles with Linear Poly (2-vinylpyridine) in Aqueous Buffers. *Materials and Manufacturing Processes* **2008**, *23*, 557–560.

(103) Polotsky, A. A.; Plamper, F. A.; Borisov, O. V. Collapse-to-Swelling Transitions in pH- and Thermoresponsive Microgels in Aqueous Dispersions: The Thermodynamic Theory. *Macromolecules* **2013**, *46*, 8702–8709, DOI: 10.1021/ma401402e.

(104) Kielland, J. Individual activity coefficients of ions in aqueous solutions. *Journal of the American Chemical Society* **1937**, *59*, 1675–1678.

Graphical TOC Entry

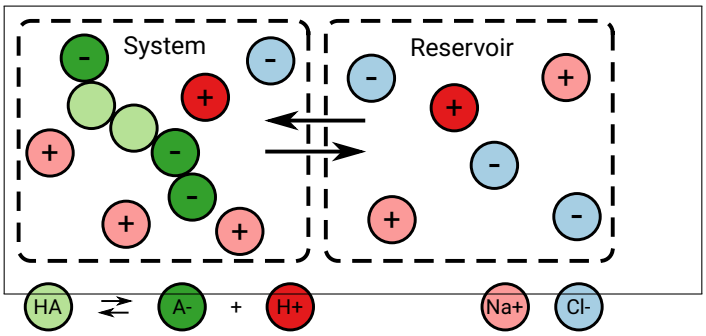

This is just a placeholder for the new TOC figure.

Supporting Information: Grand-reaction method for simulations of ionization equilibria coupled to ion partitioning

Jonas Landsgesell,[†] Pascal Hebbeker,[‡] Oleg Rud,[‡] Raju Lunkad,[‡] Peter Košovan,[*,‡] and Christian Holm[*,†]

[†]*Institute for Computational Physics, University of Stuttgart, Allmandring 3, D-70569 Stuttgart, Germany*

[‡]*Department of Physical and Macromolecular Chemistry, Faculty of Science, Charles University, Hlavova 2030, 128 43 Prague, Czech Republic*

E-mail: peter.kosovan@natur.cuni.cz; holm@icp.uni-stuttgart.de

S1 Technical details of the simulations

S1.1 Simulation protocol

The Langevin equation was integrated by a Velocity Verlet algorithm with a time step of $\delta t = 0.01\sigma(m/k_{\mathrm{B}}T)^{1/2}$ where m is the mass of the particles.*

Equilibration run consisted of 50 cycles, and each equilibration cycle consisted of $16N+10$ reaction moves, and $1000 + 2N$ MD integration steps followed by extensive additional equilibration with 1.6×10^5 reaction moves. The production run followed after the equilibration,

*Note that mass of the particles is arbitrary. All the presented results are invariant with respect to it. However, the ratio of the particle mass and energy determines the stability window of the algorithm. Also, the time evolution of the system is nonphysical, as the Monte Carlo reaction moves do not include the physical dynamics.

with each production cycle consisting of $3N + 20$ reaction moves, and $1000 + 2N$ MD integration steps. We calculated ensemble-averaged values of the observables from the configurations after each production cycle. To assess the statistical accuracy of our data, we used the correlation-corrected error estimate[S1]. The total length of the simulation was adjusted to typically yield ≈ 500 uncorrelated samples of the slowest decorrelating observable (i.e. the end-to-end distance). Depending on the system parameters, this was typically achieved within $2 \times 10^3 - 2 \times 10^4$ production cycles per simulation.

S1.2 Auxiliary simulations of the reservoir

To determine excess chemical potentials in the reservoir, we use the direct calculation by Widom particle insertion, outlined in the main text. Because all ion types in our model have identical interaction parameters, except for valency, their excess chemical potentials are the same, and depend only on the ionic strength but do not depend on the ion type. Therefore, we calculated the excess chemical potential of individual ions as one half the excess chemical potential of the ion pair.

We performed a set of auxiliary simulations of the reservoir with 400 ion pairs (Na^+ and Cl^-, 800 ions in total), and with the simulation box size set obtain the desired ionic strength. We measured excess chemical potential as a function of ionic strength, $\mu_i^{\mathrm{ex}}(I^{\mathrm{res}})$, and interpolated these data points to obtain the excess chemical potential at an arbitrary value of ionic strength within the relevant range (see Supporting Information, Section S7).

We determined the reservoir composition at a given pH and salt concentration that corresponds to a salt solution (NaCl), the pH of which was adjusted to the desired value by adding NaOH or HCl. To obtain the composition we defined the following functions:

$$\Delta\mathrm{pH}(c_{\mathrm{H^+}}^{\mathrm{res}}, c_{\mathrm{OH^-}}^{\mathrm{res}}) = \mathrm{pH} - \mathrm{pH}_{\mathrm{observed}}(c_{\mathrm{H^+}}^{\mathrm{res}}, c_{\mathrm{OH^-}}^{\mathrm{res}}) \tag{S1}$$

$$\Delta\mathrm{pOH}(c_{\mathrm{H^+}}^{\mathrm{res}}, c_{\mathrm{OH^-}}^{\mathrm{res}}) = \mathrm{p}K_{\mathrm{w}} - \mathrm{pH} - \mathrm{pOH}_{\mathrm{observed}}(c_{\mathrm{H^+}}^{\mathrm{res}}, c_{\mathrm{OH^-}}^{\mathrm{res}}) \tag{S2}$$

where pH refers to the target value, while $\mathrm{pH}_{\mathrm{observed}}$ and $\mathrm{pOH}_{\mathrm{observed}}$ are functions of $c^{\mathrm{res}}_{\mathrm{H^+}}$ and $c^{\mathrm{res}}_{\mathrm{OH^-}}$:

$$\mathrm{pH}_{\mathrm{observed}}(c^{\mathrm{res}}_{\mathrm{H^+}}, c^{\mathrm{res}}_{\mathrm{OH^-}}) = -\log_{10}(c^{\mathrm{res}}_{\mathrm{H^+}}/c^{\ominus}) + \beta\mu^{\mathrm{ex}}(I^{\mathrm{res}}(c^{\mathrm{res}}_{\mathrm{H^+}}, c^{\mathrm{res}}_{\mathrm{OH^-}}))/\ln(10) \tag{S3}$$

$$\mathrm{pOH}_{\mathrm{observed}}(c^{\mathrm{res}}_{\mathrm{H^+}}, c^{\mathrm{res}}_{\mathrm{OH^-}}) = -\log_{10}(c^{\mathrm{res}}_{\mathrm{OH^-}}/c^{\ominus}) + \beta\mu^{\mathrm{ex}}(I^{\mathrm{res}}(c^{\mathrm{res}}_{\mathrm{H^+}}, c^{\mathrm{res}}_{\mathrm{OH^-}}))/\ln(10) \tag{S4}$$

Then we expressed the reservoir ionic strength in terms of the salt concentration

$$I^{\mathrm{res}}(c^{\mathrm{res}}_{\mathrm{H^+}}, c^{\mathrm{res}}_{\mathrm{OH^-}}) = \frac{1}{2}\left(c^{\mathrm{res}}_{\mathrm{H^+}} + c^{\mathrm{res}}_{\mathrm{OH^-}} + c^{\mathrm{res}}_{\mathrm{Na^+}} + c^{\mathrm{res}}_{\mathrm{Cl^-}}\right) = c^{\mathrm{res}}_{\mathrm{salt}} + \frac{1}{2}\left(c^{\mathrm{res}}_{\mathrm{H^+}} + c^{\mathrm{res}}_{\mathrm{OH^-}} + \left|c^{\mathrm{res}}_{\mathrm{H^+}} - c^{\mathrm{res}}_{\mathrm{OH^-}}\right|\right) \tag{S5}$$

in order to obtain ΔpH and ΔpOH as a function of $c^{\mathrm{res}}_{\mathrm{H^+}}$ or $c^{\mathrm{res}}_{\mathrm{OH^-}}$, for a given value of $c^{\mathrm{res}}_{\mathrm{salt}}$ and pH. Finally, we used standard multidimensional root finding algorithms[S2] to find the roots of Equation S2, where $\Delta\mathrm{pH} = 0$ and $\Delta\mathrm{pOH} = 0$. As an initial guess to find the roots, we used the concentrations of the corresponding ideal system: $c^{\mathrm{res}}_{\mathrm{H^+}} = 10^{-\mathrm{pH}}c^{\ominus}$, $c^{\mathrm{res}}_{\mathrm{OH^-}} = 10^{\mathrm{p}K_{\mathrm{w}}-\mathrm{pH}}c^{\ominus}$.

S2 Details of the G-cpH method

In general, the G-cpH method resembles the G-RxMC method, with the difference, that the RxMC method is replaced with the cpH method. Another important difference is the role of the H^+ ions in the cpH method. In the constant-pH method, the H^+ ions generated in the reactions of Eq. 1 are treated as dummy particles whose role is to retain overall electroneutrality of the simulation box. Unlike the reaction ensemble, the acceptance probability of the constant-pH method does not explicitly depend on the number of H^+ ions in the simulation box. The H^+ ion acts just as a neutralizer that ensures overall electroneutrality of the simulation box. Therefore, the number of H^+ and OH^- ions in the simulation box can be almost arbitrary. The only requirement is that their number is sufficient to allow for the protonation reaction to take place at any moment of the simulation.

If H^+ ions are the minority species in the simulation box, then there is a risk that the protonation reaction would be prevented by the absence of explicit H^+ ions. Similar situation was the bottleneck of simulations by Rathee et al.[S3,S4], where the absence of OH^- ions prevented them from simulating at pH ≈ 7. In such case, the ionization reaction can be implemented using some other ion as neutralizer. For example one can use Na^+ ions

$$HA \rightleftharpoons A^- + Na^+ \tag{S6}$$

Because the neutralizer plays no role in the constant-pH acceptance probability, one should use the same value of equilibrium constant irrespective of the type of neutralizer (Eq. S6 or Eq. 1). The reaction in Eq. S6 can be regarded as two consecutive reactions: (1) ionization of the acid that generates the H^+ ion, and (2) exchange with the reservoir, replacing the H^+ with the Na^+ ion. By choosing an ion as neutralizer which is present in sufficient high numbers, one can fulfill the requirement, that the protonation reaction can take place at any moment of the simulation.

S3 Interaction Potentials and parameters

Ions were represented by the primitive model, characterized by the valency and effective ion size. For simplicity, the short-range interactions (excluded volume) of all particles (small ions and monomers of the polymer) were represented by the purely repulsive WCA potential[S5], with the effective particle size $\sigma = 0.355\,\mathrm{nm}$ and strength of the interaction $\epsilon = 1.0\,k_\mathrm{B}T$. The FENE potential was used to account for polymer connectivity, with the typical Kremer-Grest parameters[S6] $k_\mathrm{FENE} = 30.0\,k_\mathrm{B}T/\sigma^2$, and $R_\mathrm{max} = 1.5\sigma$. Functional forms of the interaction potentials are given in Section S3 of the Supporting Information. The electrostatic coupling strength is defined by the Bjerrum length $\lambda_\mathrm{B} = 2.0\sigma = 0.71\,\mathrm{nm}$ that approximately corresponds to aqueous solution at $T = 298\,\mathrm{K}$. We use the value of $\mathrm{p}K_\mathrm{w} = 10^{-14}$ that corresponds to the same temperature.

In the simulations all particles interact via the WCA potential[S5]:

$$E_{\mathrm{WCA}}(r) = \begin{cases} 4\epsilon\left[\left(\frac{\sigma}{r}\right)^{12} - \left(\frac{\sigma}{r}\right)^{6}\right] + \epsilon, \text{ if } r < 2^{1/6}\sigma \\ 0, \text{ else} \end{cases}$$

where r is the distance between two particles.

Bonds between particles in the polymers are introduced via the FENE potential[S6]:

$$E_{\mathrm{FENE}}(r) = -\frac{1}{2}k_{\mathrm{FENE}}R_{\mathrm{max}}^2 \ln\left(1 - \left[\frac{r}{R_{\mathrm{max}}}\right]^2\right)$$

where R_{max} is the maximal stretching of the bond, k_{FENE} a constant that defines the strength of the bond. If the particle distance r approaches ΔR_{max}, then the bond potential diverges.

The Coulomb interaction energy of two charges is given by:

$$E_{\mathrm{el}}(r) = \lambda_{\mathrm{B}} k_{\mathrm{B}} T \frac{z_1 z_2}{r} \tag{S7}$$

where z_1 and z_2 are the valencies of the two charges, $k_{\mathrm{B}}T$ the thermal energy and λ_{B} the Bjerrum length. In our simulations this interaction is handled via the P3M algorithm[S7].

S4 The Donnan Equilibrium

S4.1 Donnan potential from constrained minimization of the free energy

Express the total Gibbs free energy of the system and the reservoir as a sum of chemical potentials of each exchangeable species:

$$G = \sum_j (\mu_j^*)^{\mathrm{sys}} N_j^{\mathrm{sys}} + \sum_j (\mu_j^*)^{\mathrm{res}} N_j^{\mathrm{res}} \tag{S8}$$

where μ_j^* denotes the chemical potential of species j. We use $\sum_j$ to denote the sum which runs over all exchangeable species. For simplicity, further assume that all ionic species in the reservoir can be exchanged with the system, and the system contains additional ionic species that cannot be exchanged with the reservoir. Assume that particles cannot be created or destroyed but they can only be exchanged between the system and the reservoir, such that the total number of each species is conserved

$$N_j = N_j^{\text{sys}} + N_j^{\text{res}} = \text{const} \tag{S9}$$

and we can rewrite G in terms of N_j^{sys} only:

$$G = \sum_j (\mu_j^*)^{\text{sys}} N_j^{\text{sys}} + \sum_j (\mu_j^*)^{\text{res}} (N_j - N_j^{\text{sys}}) = \sum_j N_j^{\text{sys}} ((\mu_j^*)^{\text{sys}} - (\mu_j^*)^{\text{res}}) + N_j (\mu_j^*)^{\text{res}} \tag{S10}$$

Introduce the electroneutrality constraint in the system

$$\sum_s z_s N_s^{\text{sys}} = 0 \tag{S11}$$

Note that this sum $\sum_s$ runs over all species in the system. Provided that reservoir was electroneutral before any exchange, then Eq.S9 ensures that it remains electroneutral also after the exchange. We minimize G with respect to N_i^{sys}, introducing the Lagrange multiplier λ to account for the electroneutrality constraint:

$$0 = \frac{\partial G}{\partial N_i^{\text{sys}}} \tag{S12}$$

$$= \frac{\partial}{\partial N_i^{\text{sys}}} \left(\sum_j N_j^{\text{sys}} ((\mu_j^*)^{\text{sys}} - (\mu_j^*)^{\text{res}}) + N_j (\mu_j^*)^{\text{res}} - \lambda \sum_s z_s N_s^{\text{sys}} \right) \tag{S13}$$

$$= (\mu_i^*)^{\text{sys}} - (\mu_i^*)^{\text{res}} - \lambda z_i \tag{S14}$$

We obtain a trivial solution to Eq.S14 if $c_s^{\mathrm{sys}} = c_s^{\mathrm{res}}$ for all species s, and $\lambda = 0$. If the total charge of the non-exchangeable species in the system and in the reservoir differs, then we obtain a non-trivial solution with $\lambda \neq 0$. Introducing the Donnan potential as $\mu^{\mathrm{don}} \equiv \lambda \neq 0$, we can express the non-trivial solution

$$\lambda z_i \equiv z_i \mu^{\mathrm{don}} = ((\mu_i^*)^{\mathrm{sys}} - (\mu_i^*)^{\mathrm{res}}) \tag{S15}$$

The above equation shows that chemical potentials in the system and in the reservoir differ by the term μ^{don}, that arises in an ideal system as a consequence of the electroneutrality constraint. Furthermore, since λ is a single constant for all ions, also μ^{don} is a single constant for all ions. Eq.S15 also implies that the Donnan contributions exactly cancel within any group of exchanged ions that is overall electroneutral.

At first sight, Eq. S15 seems to break the common notion that chemical potentials of each species in the system and in the reservoir are the same. However, chemical potential of individual ions are ill-defined in a system that strictly obeys electroneutrality. On the other hand, the chemical potential of an ion pair is well-defined, and it is equal in the system and in the reservoir because the Donnan terms exactly cancel. Then one can interpret the term μ^{don} as an additional term that one needs to add to the chemical potential in order to allow for a formal definition of single-ion chemical potential in an electroneutral system.

To achieve this, consider first the conventional definition of chemical potential in a single-phase system without the Donnan contribution:

$$\mu_i^* = \mu_i^{\ominus} + \mu_i^{\mathrm{id}} + \mu_i^{\mathrm{ex}} = \mu_i^{\ominus} + k_{\mathrm{B}} T \ln(c_i/c^{\ominus}) + \mu_i^{\mathrm{ex}} \tag{S16}$$

where $\mu_i^{\ominus}$ is the reference chemical potential, μ_i^{id} is the ideal chemical potential, c_i is the concentration, $c^{\ominus}$ is the reference concentration, and μ_i^{ex} is the excess chemical potential of species i. Now, we can introduce a new definition of the (extended) chemical potential μ, that includes the Donnan contribution. Furthermore, we apply a convention that $(\mu^{\mathrm{don}})^{\mathrm{res}} = 0$ to

obtain

$$\mu_i^{\mathrm{sys}} = \mu_i^{\ominus} + (\mu_i^{\mathrm{id}})^{\mathrm{sys}} + (\mu_i^{\mathrm{ex}})^{\mathrm{sys}} + z_i\mu^{\mathrm{don}} \quad = \mu_i^{\ominus} + k_{\mathrm{B}}T\ln(c_i^{\mathrm{sys}}/c^{\ominus}) + (\mu_i^{\mathrm{ex}})^{\mathrm{sys}} + z_i\mu^{\mathrm{don}} \tag{S17}$$

$$\mu_i^{\mathrm{res}} = \mu_i^{\ominus} + (\mu_i^{\mathrm{id}})^{\mathrm{res}} + (\mu_i^{\mathrm{ex}})^{\mathrm{res}} \quad = \mu_i^{\ominus} + k_{\mathrm{B}}T\ln(c_i^{\mathrm{res}}/c^{\ominus}) + (\mu_i^{\mathrm{ex}})^{\mathrm{res}} \tag{S18}$$

With the above definitions, the extended chemical potentials of all exchangeable species are equal in the reservoir and in the system,

$$\mu_i^{\mathrm{sys}} = \mu_i^{\mathrm{res}} \tag{S19}$$

To calculate the Donnan potential, we can rewrite the electroneutrality constraint in terms of concentrations as

$$\sum_j z_j c_j^{\mathrm{sys}} = -\sum_k z_k c_k^{\mathrm{sys}} \tag{S20}$$

where the summation $\sum_k$ runs over all non-exchangeable species in the system. From Eq. S19 we obtain for all exchangeable species

$$c_i^{\mathrm{sys}} = c_i^{\mathrm{res}} \exp\left(\Delta_{\mathrm{sys-res}}\mu_i^{\mathrm{ex}} + z_i\mu^{\mathrm{don}}\right) \tag{S21}$$

where $\Delta_{I-II}\mu_i^{\mathrm{ex}} = (\mu^{\mathrm{ex}})^{II} - (\mu^{\mathrm{ex}})^{I}$. Combining the two above equations, we obtain

$$\sum_j z_j c_j^{\mathrm{res}} \exp\left(\Delta_{\mathrm{sys-res}}\mu_j^{\mathrm{ex}} + \mu^{\mathrm{don}} z_j\right) = -\sum_k z_k c_k^{\mathrm{sys}} \tag{S22}$$

which can be solved for μ^{don} if values of μ_i^{ex} are known. This shows that μ^{don} depends on the concentrations of the exchangeable species in the reservoir, on the charge concentration of the non-exchangeable species in the system, and on the difference of the excess chemical potentials of the exchangeable species in the system and the reservoir. For a system with zero excess chemical potential, we can calculate μ^{don} analytically (see below), but this is not possible in the general case.

S4.2 Classical Donnan Equilibrium

The Donnan equilibrium[S8–S10] was formulated for systems with two components: a charged species which can only exist in the system, and a monovalent salt, which is in equilibrium with a reservoir. It is also assumed that the solvent is in compressible. Here we briefly describe the Donnan equilibrium where A^- ions can only exist in the system, while Na^+Cl^- salt is in equilibrium with the reservoir. The ion partitioning is described using two assumptions:

1. The system is electroneutral

$$n_{Na^+} = n_{Cl^-} + n_{A^-} \tag{S23}$$

2. The neutral salt is treated ideally:

$$\mu_{Na^+Cl^-} = \mu_{Na^+} + \mu_{Cl^-} = \mu^{\ominus}_{Na^+} + \mu^{\ominus}_{Cl^-} + \ln\left[\frac{c^{sys}_{Na^+} c^{sys}_{Cl^-}}{c^{\ominus 2}}\right] \tag{S24}$$

Because $\{Na^+Cl^-\}$ is an electroneutral ion pair, the Donnan contributions cancel in the system and in the reservoir, (cf. Eq.S17 and Eq.S18). Eq.S24 thus attains the same for in the system and in the reservoir, and we obtain

$$(\mu_{Na^+})^I + (\mu_{Cl^-})^I = (\mu_{Na^+})^{II} + (\mu_{Cl^-})^{II} \tag{S25}$$

$$c^{sys}_{Na^+} c^{sys}_{Cl^-} = c^{res}_{Na^+} c^{res}_{Cl^-} \tag{S26}$$

$$c^{sys}_{Cl^-} / c^{res}_{Cl^-} = c^{res}_{Na^+} / c^{sys}_{Na^+} \tag{S27}$$

where we introduce a notation convention that c_i^{sys} denotes concentration of species i in the system, and c_i^{res} denotes its concentration in the reservoir. Using the electroneutrality of the reservoir, $c^{res}_{Na^+} = c^{res}_{Cl^-}$, we can express the ionic strength in the reservoir as

$$I^{res} = \left(0.5 c^{res}_{Na^+} + 0.5 c^{res}_{Cl^-}\right) \tag{S28}$$

$$= \left(c^{res}_{Na^+}\right) = \left(c^{res}_{Cl^-}\right). \tag{S29}$$

We define the partitioning coefficient ξ_i as

$$\xi_i = \frac{c_i^{\text{sys}}}{c_i^{\text{res}}} \tag{S30}$$

Note that from Equation S27 it follows that $\xi_{\text{Cl}^-} = 1/\xi_{\text{Na}^+}$. Here we use a slightly different notation than in previous work[S9,S11], which used a universal ξ', which relates to the ξ values used here as

$$\xi' = \xi_{\text{Cl}^-} = 1/\xi_{\text{Na}^+} \tag{S31}$$

We decided to use this different notation, as this way, an increase in ξ always corresponds to an increase of the concentration in the system, relative to the reservoir concentration.

Combining the above equations, we obtain the famous Donnan partitioning for the coion (Cl^-):

$$n_{\text{Cl}^-} + n_{\text{A}^-} = n_{\text{Na}^+} \tag{S32}$$

$$c_{\text{Cl}^-}^{\text{sys}} + c_{\text{A}^-}^{\text{sys}} = c_{\text{Na}^+}^{\text{sys}} \tag{S33}$$

$$I^{\text{res}}\xi_{\text{Cl}^-} + c_{\text{A}^-}^{\text{sys}} = I^{\text{res}}\xi_{\text{Na}^+} \tag{S34}$$

$$I^{\text{res}}\xi_{\text{Cl}^-} + c_{\text{A}^-}^{\text{sys}} = I^{\text{res}}/\xi_{\text{Cl}^-} \tag{S35}$$

$$\xi_{\text{Cl}^-} = -c_{\text{A}^-}^{\text{sys}}/2I^{\text{res}} \pm \sqrt{\left(c_{\text{A}^-}^{\text{sys}}/2I^{\text{res}}\right)^2 + 1} \tag{S36}$$

$$\xi_{\text{Cl}^-} = -c_{\text{A}^-}^{\text{sys}}/2I^{\text{res}} + \sqrt{\left(c_{\text{A}^-}^{\text{sys}}/2I^{\text{res}}\right)^2 + 1} \tag{S37}$$

where we regard only the positive root, as $\xi \geq 0$. We obtain the partitioning of Na^+ as

$$\xi_{\text{Na}^+} = +c_{\text{A}^-}^{\text{sys}}/2I^{\text{res}} + \sqrt{\left(c_{\text{A}^-}^{\text{sys}}/2I^{\text{res}}\right)^2 + 1} \tag{S38}$$

S4.3 Donnan equilibrium with four ionic species

Extending the Donnan Equilibrium to four ionic species in the reservoir is straightforward[S9,S11]. The relevant components are: a charged species A^- which can only exist in

the system, and four ionic species (two cations, two anions: Na^+, Cl^-, H^+, OH^-), which are in equilibrium with a reservoir. We use the same assumptions as before:

1. The system is electroneutral

$$n_{Na^+} + n_{H^+} = n_{A^-} + n_{Cl^-} + n_{OH^-} \tag{S39}$$

2. The species which can be exchanged are treated as ideal ions. Four different neutral species exists, so that we have

$$c^{sys}_{Na^+} c^{sys}_{Cl^-} = c^{res}_{Na^+} c^{res}_{Cl^-} \tag{S40}$$
$$c^{sys}_{Na^+} c^{sys}_{OH^-} = c^{res}_{Na^+} c^{res}_{OH^-} \tag{S41}$$
$$c^{sys}_{H^+} c^{sys}_{Cl^-} = c^{res}_{H^+} c^{res}_{Cl^-} \tag{S42}$$
$$c^{sys}_{H^+} c^{sys}_{OH^-} = c^{res}_{H^+} c^{res}_{OH^-} \tag{S43}$$

and therefore

$$c^{sys}_{Cl^-}/c^{res}_{Cl^-} = c^{res}_{Na^+}/c^{sys}_{Na^+} \tag{S44}$$
$$c^{sys}_{OH^-}/c^{res}_{OH^-} = c^{res}_{Na^+}/c^{sys}_{Na^+} \tag{S45}$$
$$c^{sys}_{OH^-}/c^{res}_{OH^-} = c^{res}_{H^+}/c^{sys}_{H^+} \tag{S46}$$
$$c^{sys}_{Cl^-}/c^{res}_{Cl^-} = c^{res}_{H^+}/c^{sys}_{H^+} \tag{S47}$$
$$c^{sys}_{Cl^-}/c^{res}_{Cl^-} = c^{sys}_{OH^-}/c^{res}_{OH^-} = c^{res}_{Na^+}/c^{sys}_{Na^+} = c^{res}_{H^+}/c^{sys}_{H^+} \tag{S48}$$

Using the electroneutrality of the reservoir, we have

$$I^{res} = \left(0.5c^{res}_{Na^+} + 0.5c^{res}_{H^+} + 0.5c^{res}_{Cl^-} + 0.5c^{res}_{OH^-}\right) \tag{S49}$$
$$= \left(c^{res}_{Na^+} + c^{res}_{H^+}\right) = \left(c^{res}_{Cl^-} + c^{res}_{OH^-}\right) \tag{S50}$$

We use the same definition of ξ_i as above, and note that

$$\xi_{\mathrm{OH^-}} = \xi_{\mathrm{Cl^-}} = 1/\xi_{\mathrm{H^+}} = 1/\xi_{\mathrm{Na^+}} \tag{S51}$$

so that we introduce the shorthand notations

$$\xi_- = \xi_{\mathrm{OH^-}} = \xi_{\mathrm{Cl^-}} \tag{S52}$$

$$\xi_+ = \xi_{\mathrm{H^+}} = \xi_{\mathrm{Na^+}} \tag{S53}$$

$$\xi_+ = 1/\xi_-. \tag{S54}$$

Using the electroneutrality condition we obtain the partitioning of each coion (ξ_-) as

$$c^{\mathrm{sys}}_{\mathrm{Na^+}} + c^{\mathrm{sys}}_{\mathrm{H^+}} = c^{\mathrm{sys}}_{\mathrm{Cl^-}} + c^{\mathrm{sys}}_{\mathrm{OH^-}} + c^{\mathrm{sys}}_{\mathrm{A^-}} \tag{S55}$$

$$I^{\mathrm{res}}/\xi_- = I^{\mathrm{res}}\xi_- + c^{\mathrm{sys}}_{\mathrm{A^-}} \tag{S56}$$

$$\xi_- = -c^{\mathrm{sys}}_{\mathrm{A^-}}/2I^{\mathrm{res}} + \sqrt{\left(c^{\mathrm{sys}}_{\mathrm{A^-}}/2I^{\mathrm{res}}\right)^2 + 1} \tag{S57}$$

and for the counter ions

$$\xi_+ = +c^{\mathrm{sys}}_{\mathrm{A^-}}/2I^{\mathrm{res}} + \sqrt{\left(c^{\mathrm{sys}}_{\mathrm{A^-}}/2I^{\mathrm{res}}\right)^2 + 1}. \tag{S58}$$

S4.4 Additional Results

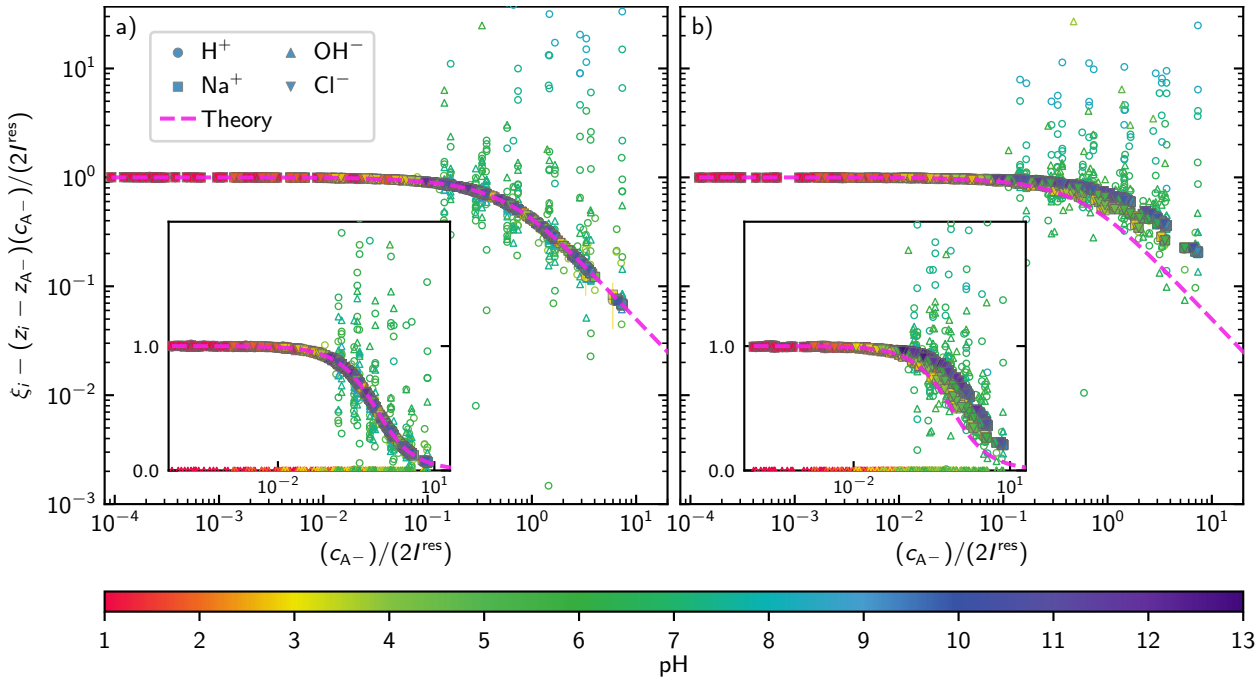

Figure S1: The data is the same as in Figure 2, except that here we do not omit any data here. Empty data points show the partitioning of ions of which (on average) less than 10 ions were in the simulation box, for which we expect finite size artifacts. This shows, that the outliers can be attributed to the finite size effects.

S5 Exclusion radius

Dealing with charged particles introduces the need for a short ranged repulsive interaction which is in our case the diverging WCA interaction. For numerical stability of the MD integration it is essential that the forces which occur during the simulation are not too high for the used time step. If the placing of new particles on MC step is completely random, then it may happen, that a new configuration is accepted where particles are placed very close to each other. This results in failure of the consecutive MD integration, because forces acting on these particles are too high for the numerical integrator.

In order to deal with this problem in a previous publication[S12] we restricted the space for particle insertions by an exclusion radius r_{excl}, such that all the insertions of particles closer than r_{excl} to another particle were not allowed. By that time the MC moves proposing the states with $r < r_{\text{excl}}$ were not directly rejected, but instead we continued proposing new

states until the distance between particles was bigger than r_{excl}. This resulted in wrong sampling, especially for systems with high density. The issue is reflected in figure 2 of that publication[S12], where the values of the excess chemical potential of the ions are below the experimental data, whereas they lie above in figure S3. In the current work this issue has been resolved by properly rejecting those moves.

S6 Required Set of Reactions

We illustrate the need to include a sufficient set of reactions by investigating a system similar to the one studied by Rathee et al.[S3,S4]. We will investigate only an ideal non-interacting system to avoid any complications due to the polyelectrolyte effect or due to short-range interactions (hydrophobicity). In particular, we show how the choice of the set of reactions affects the degree of ionization obtained in the simulation.

The studied system comprises an acid A, which can not be exchanged with a reservoir, and ion pairs K^+OH^- and Na^+Cl^-, both of which can be exchanged with a reservoir. First, we consider the same set of reactions as was used by Rathee et al.[S4]

$$A^- \rightleftharpoons HA + OH^-, \qquad K = K_w/K_A \tag{S59}$$

$$\emptyset \rightleftharpoons Na^+ + Cl^- \tag{S60}$$

$$\emptyset \rightleftharpoons K^+ + OH^- \tag{S61}$$

They formulated the acid dissociation by Reaction S59, because they simulated a system at basic conditions. In such case, the H^+ ions can be safely neglected. In this set of reactions, it is not possible to exchange K^+ for Na^+, or OH^- for Cl^-. Therefore, this set of reactions represents a setup, where KOH and NaCl are present in two different reservoirs, which can not exchange ions. However, all four ions, $K^+Na^+Cl^-OH^-$ are present in the system. In a more realistic setup, both reservoirs should exchange all small ions with the system, that

would be equivalent to coupling the system with a single reservoir containing a mixture of KOH and NaCl. The set of reactions given above is insufficient to simulate coupling with such reservoir.

Second, we consider a sufficient set of reactions, obtained by adding of the following to reaction to the above set:

$$\mathrm{OH^-} \rightleftharpoons \mathrm{Cl^-} \tag{S62}$$

$$\mathrm{K^+} \rightleftharpoons \mathrm{Na^+} \tag{S63}$$

This set of reactions represents coupling with a single reservoir containing all four ions, $\mathrm{K^+Na^+Cl^-OH^-}$. Note that Reactions S59–S62 already constitute a sufficient set, and Reaction S63 is redundant. However, we also include Reaction S63 in the set because it improves sampling efficiency.

The simulated system initially consists of 121 base particles ($\mathrm{A^-}$) with concentration $c_{\mathrm{pol}} \approx 0.05\,\mathrm{M}$, and equal amount of $\mathrm{K^+}$ ions, in a cubic simulation box with periodic boundary conditions. The concentration of NaCl in the reservoir was set to $c_{\mathrm{salt}}^{\mathrm{res}} = 0.01\,\mathrm{M}$ and the concentration of KOH in the reservoir was set to $c_{\mathrm{KOH}} = 0.002\,\mathrm{M}$. The acidity constant ($\mathrm{p}K_{\mathrm{A}}$) was varied between 8.8 to 13.8 while keeping a constant value of pH = 11.3, determined by the concentration of KOH. These parameters correspond to the ones used by Rathee et al.[S4].

Figure S2 shows that the shift in the titration curve obtained using the insufficient set is larger than that obtained using the sufficient set of reactions. In the insufficient set of reactions, the ionization reaction is coupled only with the KOH reservoir because the Reaction S59 is not linked to Reaction S61 by any component. Because the Donnan effect on the ionization reaction is controlled by the $\mathrm{OH^-}$ concentration in the KOH reservoir, it depends on the ratio $c_{\mathrm{A^-}}/2c_{\mathrm{KOH}}$. With the insufficient set of reactions, the shift in the titration curve due to the Donnan effect is approximately ≈ 1.0 units of $\mathrm{p}K_{\mathrm{A}}$.

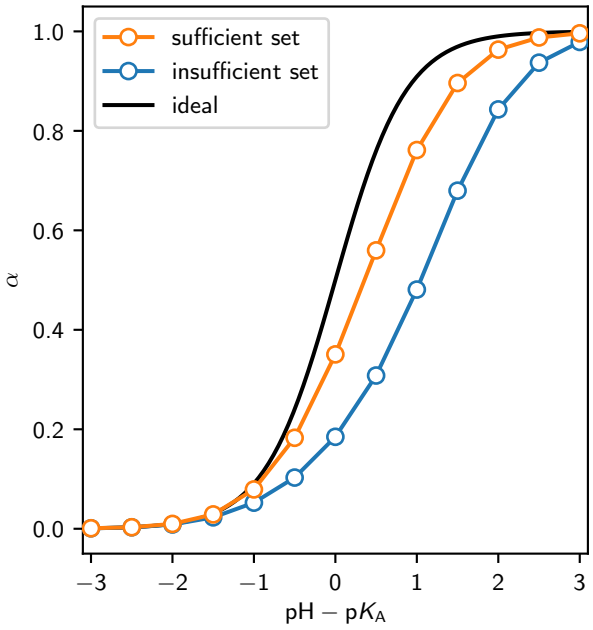

Figure S2: The degree of ionization as a function of pH − pK_A, (titration curves) obtained by simulating an ideal system using the insufficient and the sufficient set of reactions.

When using the sufficient set, the KOH and the NaCl reservoirs are mutually coupled, and the Reaction S59 is coupled with this combined reservoir. Therefore, the Donnan effect on the ionization reaction depends on the ratio $c_{A^-}/2(c_{KOH} + c^{res}_{salt})$, and is smaller than the Donnan effect in the insufficient set. Therefore, the shift in the titration curve due to the Donnan effect in the sufficient set of reactions is also smaller than in the insufficient set, roughly 0.4 units of pK_A.

S7 Excess chemical potential in the reservoir

The excess chemical potential of 400 NaCl ion pairs (800 ions) at different box volumes was determined via the Widom insertion method as described in the main text. For a Bjerrum length of $l_{Bjerrum} = 0.71\,nm$ we obtained the results shown in figure S3. Note that those results do not suffer from previously undiscovered artifacts from wrong sampling of the phase space in[S12].

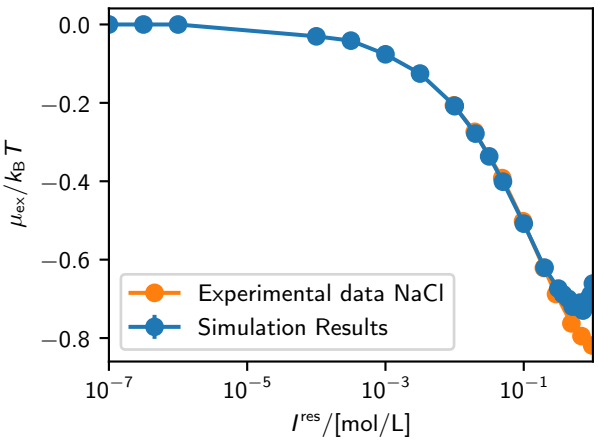

Figure S3: Excess chemical potential as a function of (reservoir) ionic strength. Error bars smaller than symbol size. Orange points mark experimental results form the activity coefficients provided by[S13] and[S14].

S8 Titration Curve

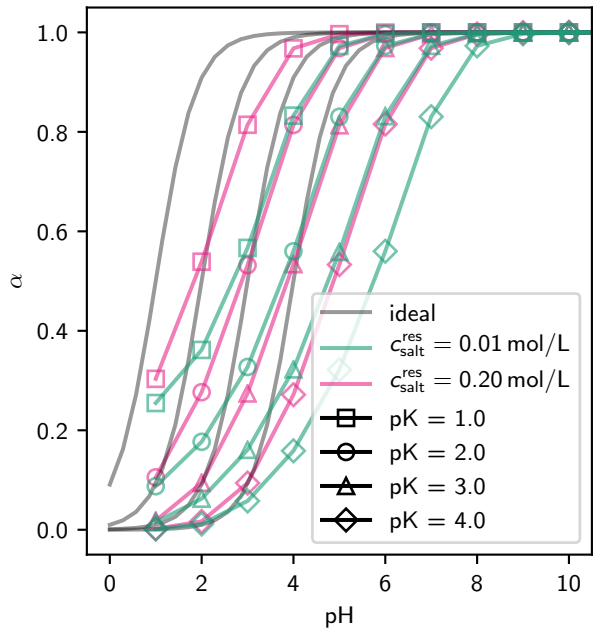

Figure S4: Ionization degree of the polyelectrolyte as a function of pH at various salt concentrations in the reservoir, and various acidity constants of the polymer, as indicated in the legend. Error bars are smaller than the point size.

S8.1 Validation of the determined chemical potentials in the reservoir

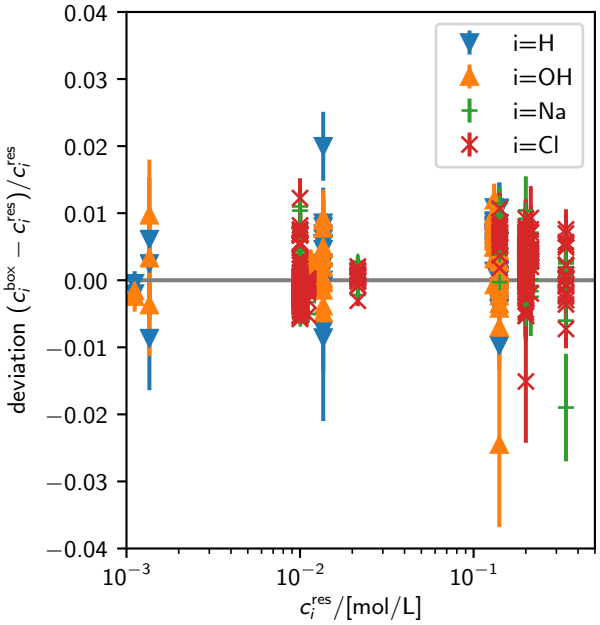

Figure S5: Relative deviation of the ion concentrations inside the simulation box and in the reservoir.

In the first step, we verify that the reservoir chemical potentials determined using the procedure described in the main text lead to the desired concentrations. We start with an initially empty simulation box, and simulate exchange of ions with the reservoir using the determined chemical potentials. We performed the simulations for all combinations of the parameters: pH $\in \{1, 2, \ldots, 13\}$, $c_{\text{salt}}^{\text{res}} \in \{0.01, 0.2\}$ M, and various simulation box lengths between $\text{box}_\text{l} \in \{6.53, \ldots, 25.56\}$ nm. In Figure S5 we show that the concentration of ions in the box, c_i^{sys} coincides with the expected reservoir concentration within 1%. Results yielding less than 10 particles in the simulation box were omitted because they are affected by finite-size effects. Deviations of all the results shown in Figure S5 are within the estimated statistical accuracy, supporting the validity of our algorithm.

S9 Comparison with a closed system

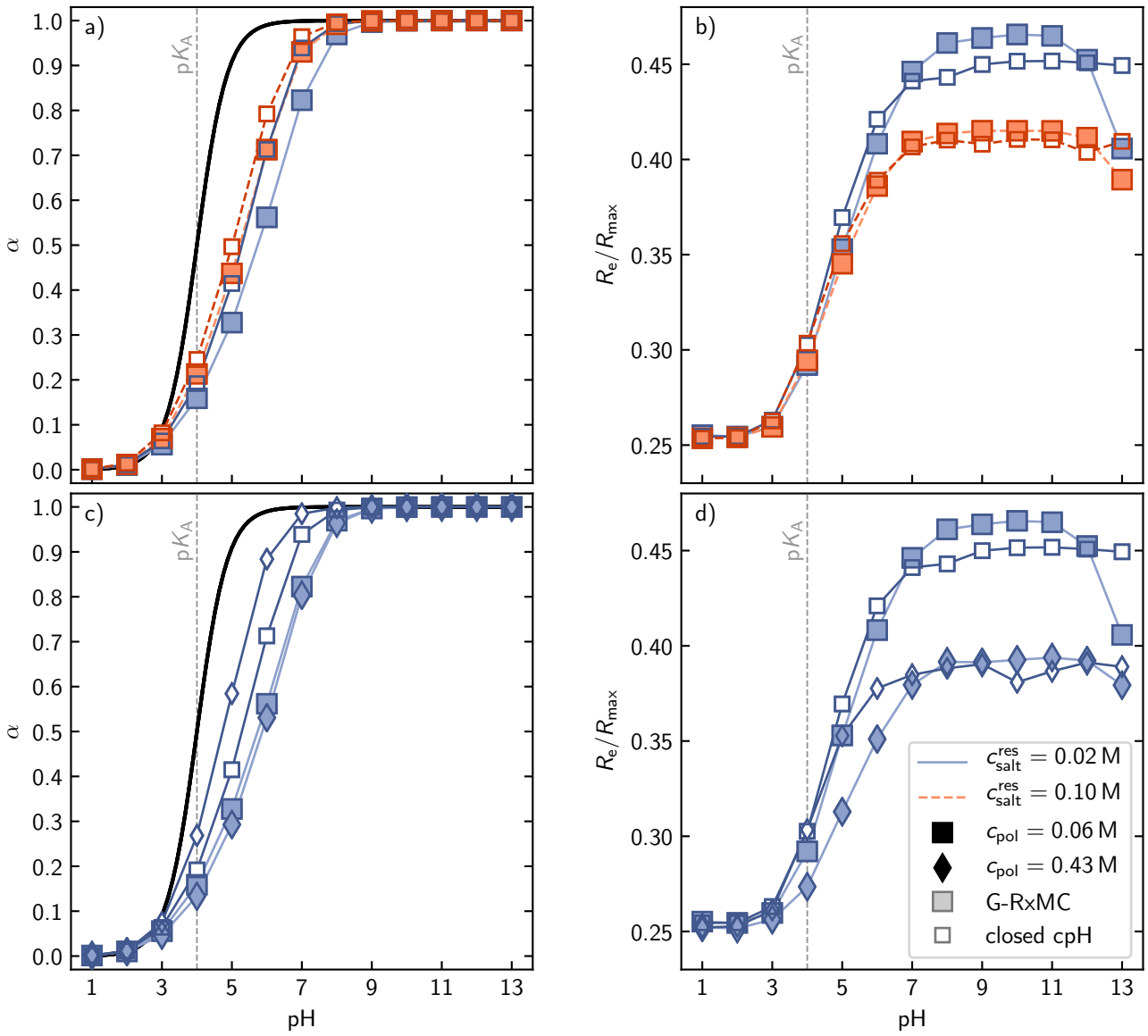

Figure S6: End-to-end distance of the weak polyelectrolyte chain with $pK_A = 4.0$ as a function of pH. To discern the polyelectrolyte effect and the Donnan effect, we compare simulations using the Grand-reaction method with constant-pH simulations at a fixed amount of added salt (closed system). Salt concentrations in the reservoir and monomer concentrations are indicated in the legend. Error bars are on the order of the point size.

To discern the effect of coupling the system to a reservoir, we compare in Figure S6 the Grand-reaction ensemble simulations of open system with constant-pH simulations of a closed system at a fixed amount of added salt. Most features of this figure were described in the

main text, when comparing G-RxMC and G-cpH simulations. Two additional effects appear when comparing open-system G-RxMC and closed-system cpH simulations. At pH $\approx$ 9 the polyelectrolyte is fully charged but the open-system simulations predict a higher chain swelling because the Donnan partitioning makes ionic strength in the open system lower than in the closed system. Confer Figure S7 to see this effect visualized. At pH $\gtrsim$ 12 the ionic strength is dominated the by the OH^- ions, and it increases with increasing pH. This leads to de-swelling of the chain at high pH. As has been pointed out earlier,[S15] this de-swelling at high pH is missing in the closed-system cpH simulations because the OH^- ions are not treated explicitly in the cpH method.

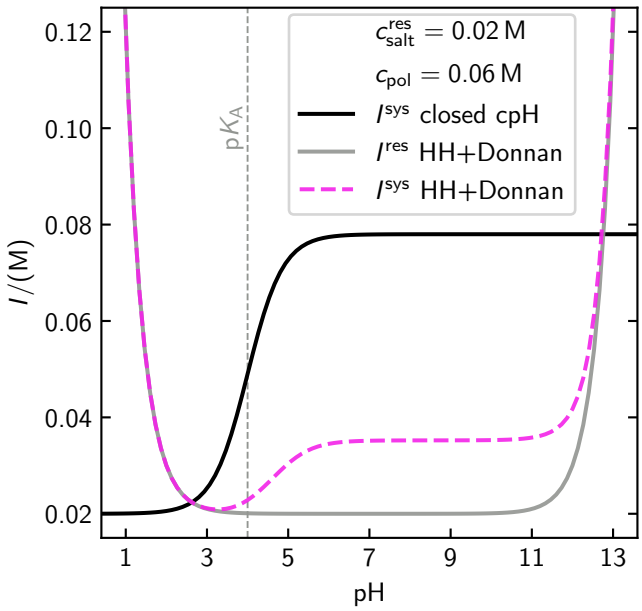

Figure S7: Ionic strength as a function of pH in an ideal HH+Donnan system, as one would encounter in an ideal G-RxMC simulation, compared to a closed system with constant amount of added salt, as one would encounter in a closed-system cpH simulation of a closed system. The ionic strength in the HH+Donnan system (I^{sys}), is always higher or equal to ionic strength in the corresponding reservoir (I^{res}). At intermediate pH, ionic strength in the closed-system cpH simulation is higher than both, I^{sys} and I^{res}, because the neutralizer in the closed system can not be partitioned to any reservoir. At extreme pH the ionic strength is dominated by the H^+ and OH^- ions. In such a case, ionic strength in the HH+Donnan setup is higher than in the closed-system cpH simulation because the closed-system cpH simulation does not explicitly include all H^+ ions.

References

(S1) Janke, W. Statistical Analysis of Simulations: Data Correlations and Error Estimation. *Quantum Simulations of Complex Many-Body Systems: from Theory to Algorithms* **2002**, 423–445.

(S2) Jones, E.; Oliphant, T.; Peterson, P.; others, SciPy: Open source scientific tools for Python. 2001; `https://scipy.org/`.

(S3) Rathee, V. S.; Sidky, H.; Sikora, B. J.; Whitmer, J. K. Role of Associative Charging in the Entropy–Energy Balance of Polyelectrolyte Complexes. *Journal of the American Chemical Society* **2018**, *140*, 15319–15328.

(S4) Rathee, V.; Sidky, H.; Sikora, B.; Whitmer, J. Explicit Ion Effects on the Charge and Conformation of Weak Polyelectrolytes. *Polymers* **2019**, *11*, 183.

(S5) Weeks, J. D.; Chandler, D.; Andersen, H. C. Role of Repulsive Forces in Determining the Equilibrium Structure of Simple Liquids. *The Journal of Chemical Physics* **1971**, *54*, 5237.

(S6) Grest, G. S.; Kremer, K. Molecular dynamics simulation for polymers in the presence of a heat bath. *Physical Review A* **1986**, *33*, 3628–31.

(S7) Eastwood, J. W.; Hockney, R. W.; Lawrence, D. N. P3M3DP–The three-dimensional periodic particle-particle/ particle-mesh program. *Computer Physics Communications* **1980**, *19*, 215–261.

(S8) Donnan, F. G. The Theory of Membrane Equilibria. *Chemical Reviews* **1924**, *1*, 73–90.

(S9) Ricka, J.; Tanaka, T. Swelling of ionic gels: quantitative performance of the Donnan theory. *Macromolecules* **1984**, *17*, 2916–2921.

(S10) Philipse, A.; Vrij, A. The Donnan equilibrium: I. On the thermodynamic foundation of the Donnan equation of state. *Journal of Physics: Condensed Matter* **2011**, *23*, 194106.

(S11) Rud, O.; Borisov, O.; Košovan, P. Thermodynamic model for a reversible desalination cycle using weak polyelectrolyte hydrogels. *Desalination* **2018**, *442*, 32–43.

(S12) Košovan, P.; Richter, T.; Holm, C. Modeling of Polyelectrolyte Gels in Equilibrium with Salt Solutions. *Macromolecules* **2015**, *48*, 7698–7708.

(S13) Truesdell, A. H. Activity Coefficients of Aqueous Sodium Chloride from 15° to 50°C Measured with a Glass Electrode. *Science* **1968**, *161*, 884–886.

(S14) Prausnitz, J. M.; Lichtenthaler, R. N.; de Azevedo, E. G. *Molecular Thermodynamics of Fluid Phase Equilibria*; Prentice Hall, 1999.

(S15) Landsgesell, J.; Holm, C.; Smiatek, J. Simulation of weak polyelectrolytes: A comparison between the constant pH and the reaction ensemble method. *The European Physical Journal Special Topics* **2017**, *226*, 725–736.